Design, synthesis, and pharmacological evaluation of 4- or 6-phenyl-pyrimidine derivatives as novel and selective Janus kinase 3 inhibitors

Lei Shu, Chengjuan Chen, Xueting Huan, Hao Huang, Manman Wang, Jianqiu Zhang, Yile Yan, Jianming Liu, Tiantai Zhang, Dayong Zhang

PII: S0223-5234(20)30115-X

DOI: https://doi.org/10.1016/j.ejmech.2020.112148

Reference: EJMECH 112148

To appear in: *European Journal of Medicinal Chemistry*

Received Date: 30 November 2019

Revised Date: 13 February 2020

Accepted Date: 13 February 2020

Please cite this article as: L. Shu, C. Chen, X. Huan, H. Huang, M. Wang, J. Zhang, Y. Yan, J. Liu, T. Zhang, D. Zhang, Design, synthesis, and pharmacological evaluation of 4- or 6-phenyl-pyrimidine derivatives as novel and selective Janus kinase 3 inhibitors, *European Journal of Medicinal Chemistry* (2020), doi: https://doi.org/10.1016/j.ejmech.2020.112148.

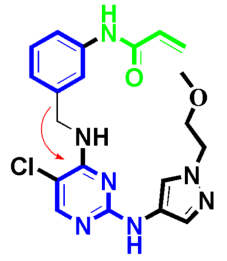

Covalent JAK3 Inhibitor

Optimization

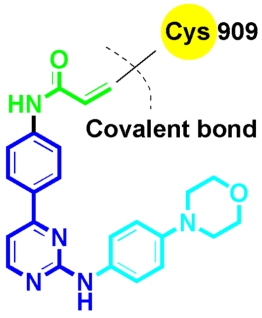

compound 12

IC_{50} = 1320/1000/1.7 nM

JAK1/JAK2/JAK3

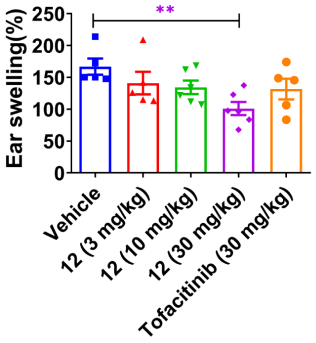

12 inhibited oxazolone-induced delayed type hypersensitivity reaction

Design, synthesis, and pharmacological evaluation of 4- or 6-phenyl-pyrimidine derivatives as novel and selective Janus kinase 3 inhibitors

Lei Shu [a,1], Chengjuan Chen [b,1], Xueting Huan [a], Hao Huang [a], Manman Wang [a], Jianqiu Zhang [a], Yile Yan [a], Jianming Liu [a], Tiantai Zhang [b,**], Dayong Zhang [a,*]

[a] *Institute of Pharmaceutical Science, China Pharmaceutical University, Nanjing 210009, PR China*

[b] *State Key Laboratory of Bioactive Substance and Function of Natural Medicines, Institute of Materia Medica, Chinese Academy of Medical Sciences and Peking Union Medical College, Beijing 100050, PR China*

[*] **Corresponding author.** Institute of Pharmaceutical Science, China Pharmaceutical University, Nanjing 210009, PR China.

[**] **Corresponding author.** State Key Laboratory of Bioactive Substance and Function of Natural Medicines, Institute of Materia Medica, Chinese Academy of Medical Sciences and Peking Union Medical College, Beijing 100050, China.

E-mail address: cpuzdy@163.com; ttzhang@imm.ac.cn (Tiantai Zhang).

[1] These authors contributed equally to this work.

Abstract

As non-receptor tyrosine kinases, Janus kinases (JAKs) have become an attractive target for the treatment of autoimmune diseases and cancers. JAKs play a pivotal role in innate immunity, inflammation, and hematopoiesis by mediating the signaling of numerous cytokines, growth factors, and interferons (IFNs). Selective inhibitors of a variety of JAK members are expected to inhibit pro-inflammatory cytokine-mediated inflammation and immune responses, while preventing targeting other subtypes of JAKs. In this work, poorly selective compounds based on 4- or 6-phenyl-pyrimidine derivatives have been improved to highly potent and selective compounds by designing a covalent binding tether, which attaches to the unique cysteine (Cys909) residue in JAK3. Compound **12** exhibited potent JAK3 inhibitory activity (IC_{50} = 1.7 nM) with an excellent selectivity profile when compared to the other JAK isoforms (> 588-fold). In a cellular assay, compound **12** strongly inhibited JAK3-dependent signaling and T cell proliferation. Moreover, *in vivo* data revealed that compound **12** significantly suppressed oxazolone (OXZ)-induced delayed hypersensitivity responses in Balb/c mice. Compound **12** also displayed decent pharmacokinetic properties and is suitable for *in vivo* use. Taken together, these results indicated that compound **12** may be a promising tool compound as a selective JAK3 inhibitor for treating autoimmune diseases.

Keywords: Autoimmune diseases; Covalent JAK3 inhibitors; Cys909; Janus kinase; 4- Or 6-phenyl-pyrimidine derivatives

1. Introduction

Janus kinases (JAK1, JAK2, JAK3, and TYK2) are a small family of non-receptor tyrosine kinases that are essential for mediating the signaling cascade that is associated with multiple cytokines by activating signal transducer and activator transcription (STAT) [1]. The JAK-STAT pathway is considered as an evolutionarily conserved signaling pathway involved in the regulation of immune and inflammatory

disease [2]. Binding of cytokines with their distinct receptor is the trigger for activation of JAKs, and upon activation STATs bind to phosphorylated cytokine receptors and undergo phosphorylation by JAKs [3]. Subsequently, dimerized STATs translocate to the nucleus and drive gene transcription, thereby regulating the immune system and inflammatory responses [4]. With the first US Food and Drug Administration (FDA)-approved pan-JAKs small molecule inhibitor tofacitinib [5,10-11] for the treatment of rheumatoid arthritis (RA), the development of small molecule JAK inhibitors became attractive for treatment of autoimmune and inflammatory diseases.

In recent years, significant research efforts have been performed towards the discovery of inhibitors of JAK kinases. As shown in Fig. 1 and Table 1, several small-molecule inhibitors are current in the clinical or preclinical stage for the treatment of autoimmune diseases, various cancers, and myeloproliferative disorders [5-16]. For the first-generation of non-selective JAKs inhibitors that have been proven safe and efficacious, their broad inhibiting spectrum for cytokines inevitably leads to side effects by inhibiting many factors that can drive immunopathology. However, the next generation selective JAKs inhibitors are expected to be developed and prevent targeting other subtypes of JAKs. In August 2019, the selective JAK1 inhibitor upadacitinib [12-14], as a second-generation JAKs inhibitor, was first approved by the US FDA for the treatment of RA. PF-06651600 [15,16] has been reported as a selective JAK3 inhibitor that has been used in clinical trials.

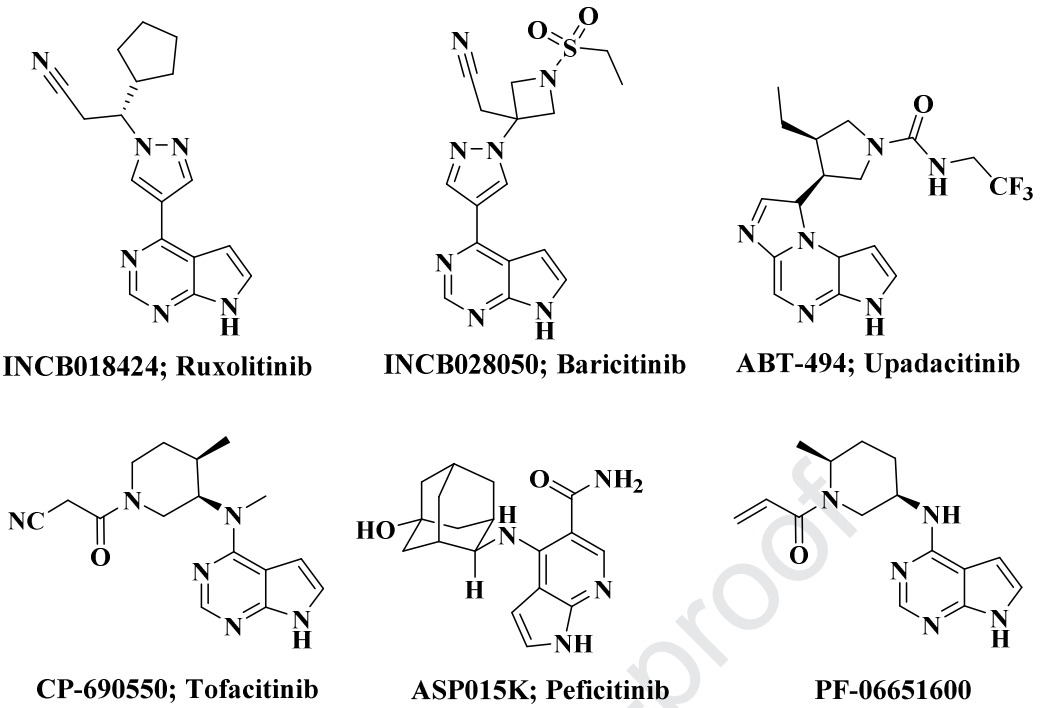

Fig. 1. Chemical structures of JAK inhibitors.

Table 1.
The selectivity of JAK inhibitors in a cell-free enzyme assay.

Compound	IC_{50}[a](nM)			JAK3/JAK2[b]	JAK3/JAK1[c]
	JAK3	JAK2	JAK1		
Ruxolitinib [6]	>400	3	3	>133	>133
Baricitinib [7]	>400	6	6	>67	>67
Upadacitinib [8]	2304	120	47	19	49
Peficitinib [9]	0.71	5.0	3.9	-	-
Tofacitinib[d]	1	20	112	-	-
PF-06651600 [15]	33	>10000	>10000	-	-

[a] IC_{50} against JAK3, JAK2, JAK1 in enzyme assay.

[b] Fold selectivity derived from JAK3/JAK2 enzyme IC_{50}.

[c] Fold selectivity derived from JAK3/JAK1 enzyme IC_{50}.

[d] Tofacitinib is originally described as being selective for JAK3 [10], however it was later proven to be a pan-JAK inhibitor [11].

Among members of the JAKs family, JAK3 exhibited predominant expression in the hematopoietic system versus other JAKs, and were ubiquitously expressed in a variety of cell types [17]. Another feature of JAK3 is that it is required for cytokine signaling, including IL-2, IL-4, IL-7, IL-9, IL-15, and IL-21, which act through relative receptors that possess the common gamma chain (γc) cytokines receptor

subunit [18]. Cytokine signaling through the γc receptor is essential for normal activity and function of the immune system [19]. In humans, loss of function mutation leading to JAK3 deficiency in γc results in severe combined immunodeficiency (SCID) [20]. A selective JAK3 inhibitor should only block common γc cytokine signaling to resulting in much narrower spectrum of cytokine activity compared to first-generation non-selective inhibitors and concomitant prevention of some the side effects. Human JAK3 has a unique cysteine residue (Cys909), which is replaced with a serine residue at the equivalent position in the other three isoforms of JAK1, JAK2, and TYK2 [21]. In crystal structure, this feature gives the opportunity to design a selective inhibitor for JAK3. Based on the difference of Cys909, targeting the Cys909 ATP-competitive binding site in a covalent manner would be an optimized strategy [22]. Recently, several selective JAK3 inhibitors have been reported to bind the Cys909 site with a covalent bond formation, leading to irreversible inhibition and high selectivity, including PF-06651600, which was reported to irreversibly covalently bind Cys909 in JAK3 [16,23]. Based on the essential role in the immune system as well as the crystal structure feature, JAK3 has been considered as a potential target for the treatment of autoimmune and inflammatory diseases.

In our previous study, we reported a series of compounds, including the bicyclic structure of pyrrolopyrimidine or pyrazolopyrimidine targeting JAKs, however, their inhibitory potency and selectivity need to be further improved [24-27]. Herein, we aimed to generate potent substituted pyrimidine-based inhibitors that exploit an acrylamide electrophile to form a covalent bond with Cys909 in JAK3. In this study, 4- Or 6-phenyl-pyrimidine derivatives as potent JAK3 inhibitors were designed and synthesized (Fig. 2). Covalent JAK3 inhibitor **(1)** has excellent biological activities against JAK3, both *in vitro* and *in vivo* [23]. Furthermore, guided by the structure of CYT-387 [28,29] and *N*-(3-(7*H*-pyrrolo[2,3-d]pyrimidin-4-yl)phenyl) acrylamide **(3)** [15], new molecules (**1**-**39**) were designed by further optimization. Our studies showed that compound **12** had significant potent JAK3 inhibitory activity and

selectivity. Therefore, in this study, we report the design, synthesis, and structure-activity relationship (SAR) of 4- or 6-phenyl-pyrimidine JAK inhibitors.

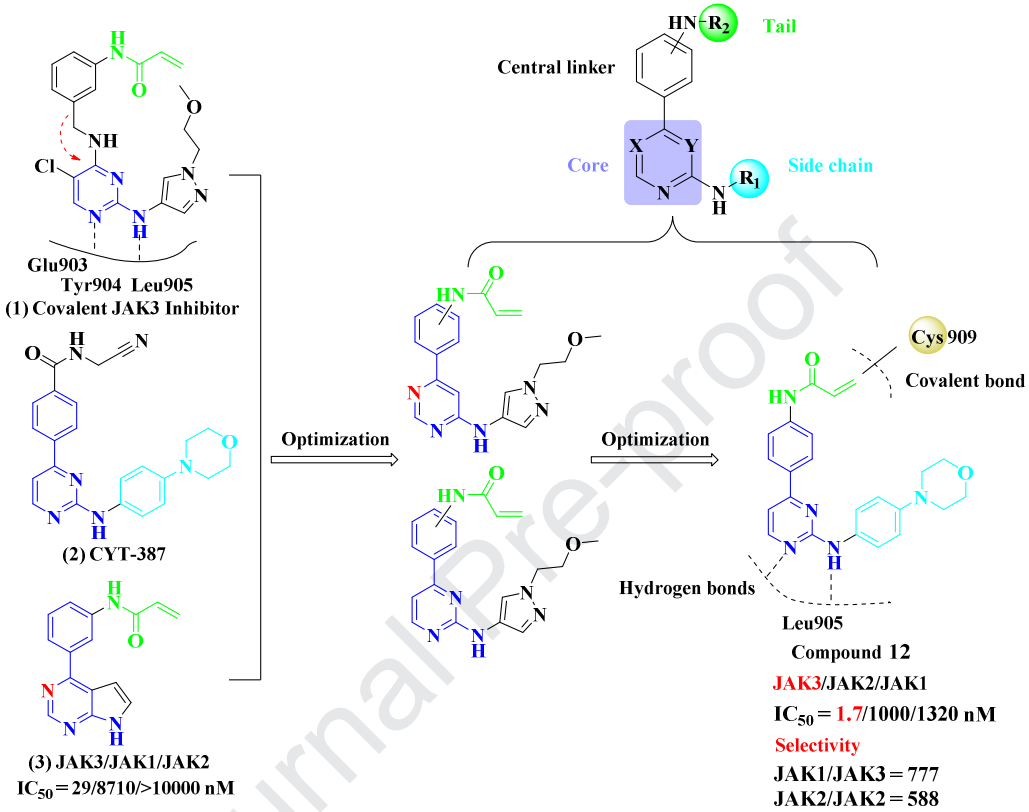

Fig. 2. Design of selective JAK3 inhibitors.

2. Results and discussion

2.1. Chemistry

A series of 4- or 6-phenyl-pyrimidine derivatives and intermediates were synthesized according to the pathways described in Schemes 1-4 (see Scheme 4, supplementary material).

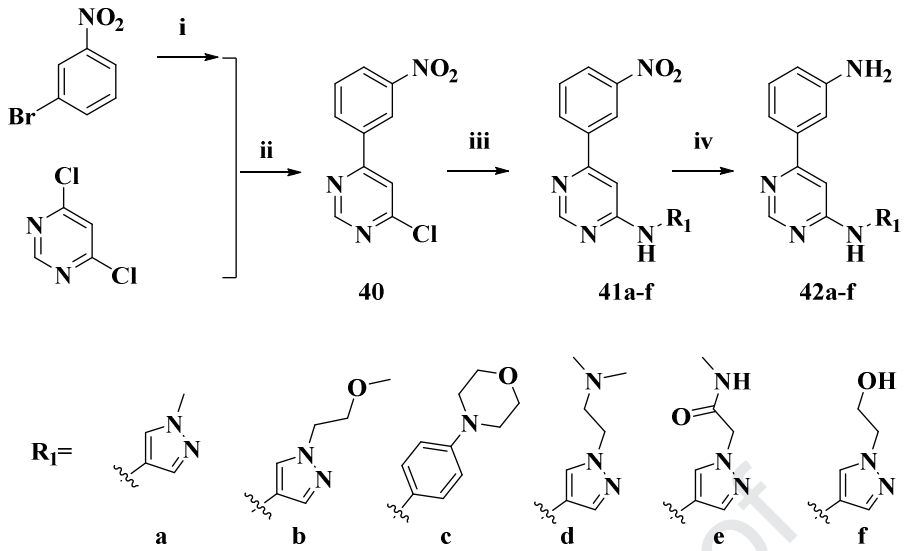

Scheme 1. Reagents and conditions: (i) bis(pinacolato)diboron, 1,4-dioxane/H_2O, $Pd(PPh_3)_4$, KOAc, 100 °C, 12 h; (ii) 1,4-dioxane/H_2O, $Pd(PPh_3)_4$, K_2CO_3, 100 °C, 12 h; (iii) amine, DIEA, isopropanol, 82 °C, 6h; (iv) Pd/C, hydrazine hydrate, EtOH, 100 °C, 2h.

As presented in Scheme 1, 3-bromo-nitrobenzene reacted with bis(pinacolato)diboron, then commercially available 4,6-dichloropyrimidine was treated with benzene pinacol borate to provide intermediate **40** at moderate yield (74%). Next, intermediate **40** was treated with several types of amines that were prepared as previously reported [24] for R_1 to produce 6-phenyl-pyrimidine amine **41a-f** under alkaline conditions. Treatment of compounds **41a-f** with 85% hydrazine hydrate under nitrogen and Pd/C catalysis provided compounds **42a-f**.

Intermediates **43**, **46**, and **49** were prepared following a synthetic procedure of that was similar to that of compound **40** (see Scheme 4, supplementary material).

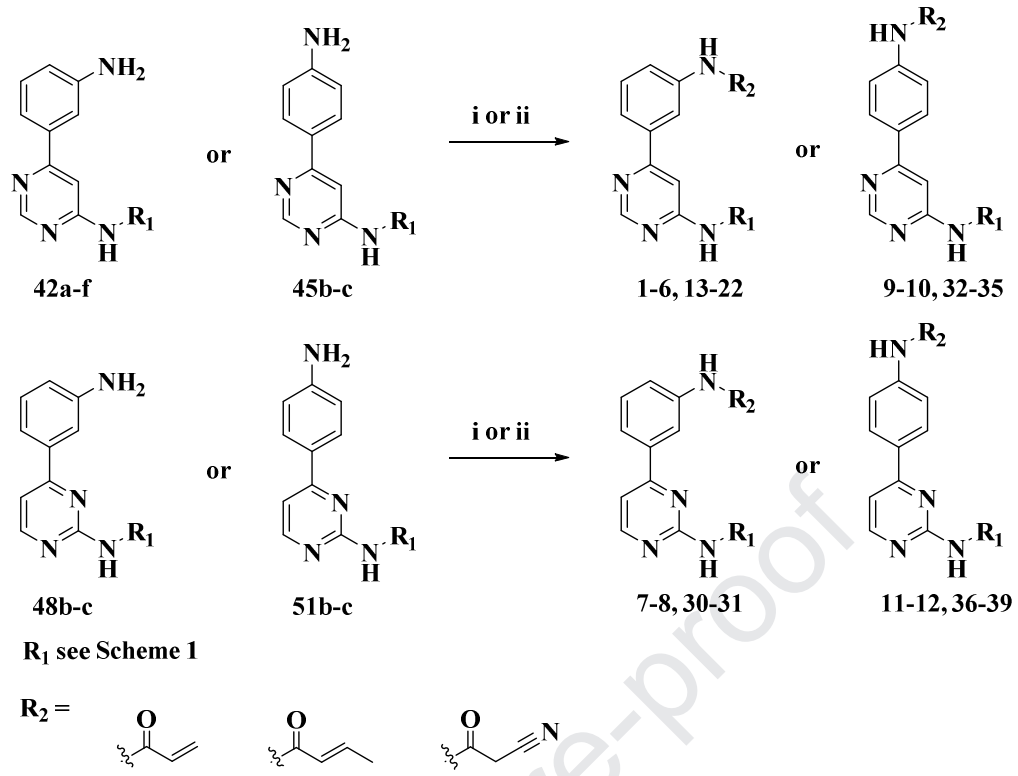

Scheme 2. Reagents and conditions: (i) acyl chlorides, THF, 0 °C to room temperature (RT), 30min; (ii) cyanoacetic acid, HATU, DIEA, THF, 16h.

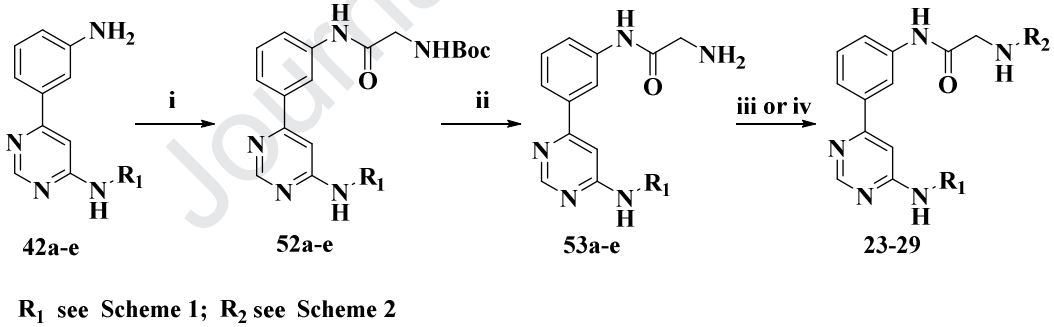

Scheme 3. Reagents and conditions: (i) Boc-glycine, EDCI, HOBT, DIEA, DCM, 8h; (ii) TFA, DCM, 5h; (iii) acyl chlorides, THF, 0 °C to room temperature (RT), 30min; (iv) cyanoacetic acid, HATU, DIEA, THF, 16h.

As shown in Scheme 3, intermediates **42a-e** were condensed with Boc-glycine to produce compounds **52a-e**. Subsequently, Boc deprotection using TFA in DCM cleanly generate compounds **53a-e** at near quantitative yield. The target compounds were prepared as presented in Scheme 2 and 3, which involved two types of reactions. First, intermediates were reacted with acyl chlorides to generate the desired

compounds under basic conditions. Subsequently, intermediates were treated with cyanoacetic acid using standard HATU conditions to generate compounds at good yield as previously reported [24].

2.2. In vitro enzymatic inhibitor activities

All newly synthesized compounds were evaluated for their activity against JAK enzymes using a Homogenous Time-Resolved Fluorescence (HTRF) Kin EASE-TK assay system. For comparison, the activity of pan JAK inhibitor tofacitinib, was also evaluated using the same procedure.

In this study, the inhibitory activity of newly synthesized compounds was evaluated using human JAK1, JAK2, JAK3, and TYK2 enzymes. To approach this optimization in a systematic fashion, this chemotype of target compounds was divided into four moieties, core (4, 6- or 2, 4-disubstituted pyrimidine), side chain (R_1), tail (R_2) and the linkage between core and tail. Furthermore, the side chain and tail varied sequentially. *In vitro*, the preliminary screening indicated that some derivatives showed good JAK3 inhibitory activity and selectivity compared with positive controls. The IC_{50} values obtained in JAK enzyme assays are summarized in Tables 2 and 3.

Table 2.
SARs of side chains (R_1)

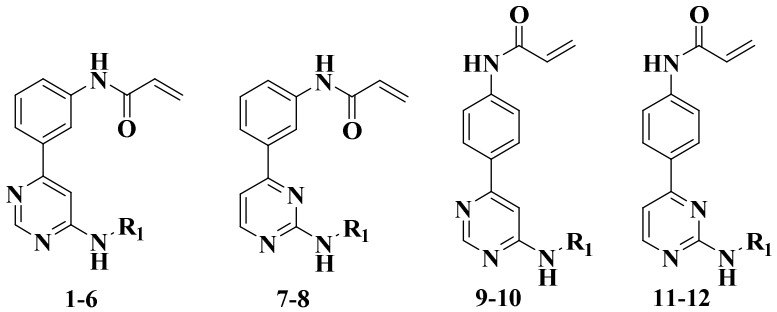

1-6 **7-8** **9-10** **11-12**

Compd	R_1	IC_{50}[a] (nM)			
		JAK3	JAK2 JAK2/JAK3[b]	JAK1 JAK1/JAK3[c]	TYK2 TYK2/JAK3[d]
1		303	2237 [7]	657 [2]	ND[e] -
2	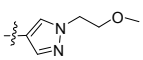	101	2852 [28]	568 [6]	ND[e] -

3	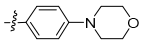	183	2043 [11]	1107 [6]	ND[e] -
4	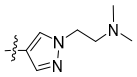	309	>3000 -	731 [2]	ND[e] -
5	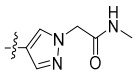	138	ND[e] -	840 [6]	ND[e] -
6	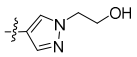	599	2588 [4]	ND[e] -	ND[e] -
7	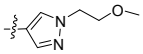	**55**	1286 [23]	1102 [20]	2871 [52]
8	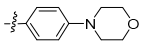	30	1796 [60]	2119 [71]	2439 [30]
9	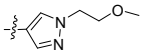	67	>3000 -	1658 [25]	>3000 -
10	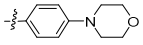	112	1569 [14]	961 [9]	ND[e] -
11	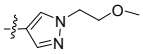	**9.1**	1079 [119]	1562 [172]	>3000 -
12	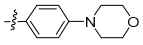	**1.7**	1000 **[588]**	1320 **[777]**	2783 [1637]
Tofacitinib		0.9	1.5 [1.7]	1.3 [1.1]	35.5 [39.4]

[a] IC_{50} values are the average of duplicate experiments.

[b] Fold selectivity derived from JAK2/JAK3 enzyme IC_{50}.

[c] Fold selectivity derived from JAK1/JAK3 enzyme IC_{50}.

[d] Fold selectivity derived from TYK2/JAK3 enzyme IC_{50}.

[e] ND = not determined.

Table 3.

SARs of side chains (R_2)

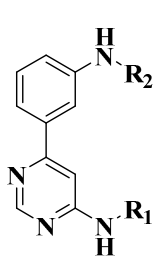

13-29

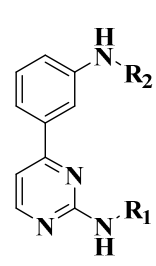

30-31

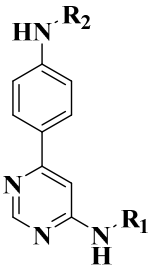

32-35

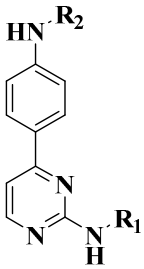

36-39

Compd	**R_1**	**R_2**	**IC_{50}[a] (nM)**			
			JAK3	**JAK2** **JAK2/JAK3[b]**	**JAK1** **JAK1/JAK3[c]**	**TYK2** **TYK2/JAK3[d]**
13			567	2761 [5]	1521 [3]	ND[e] -

14		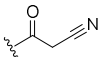	145	ND[e] -	854 [6]	ND[e] -
15	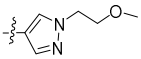		29	2580 [89]	1286 [44]	>3000 -
16	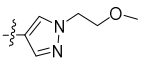	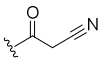	65	587 [9]	322 [5]	2264 [35]
17	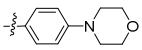		35	2129 [61]	2876 [82]	>3000 -
18	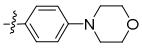	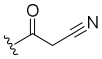	170	734 [4]	1861 [11]	ND[e] -
19	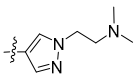		67	1886 [28]	899 [13]	ND[e] -
20	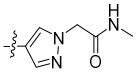		92	1109 [12]	ND[e] -	ND[e] -
21	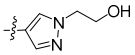		221	2808 [13]	2443 [11]	ND[e] -
22	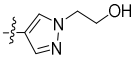	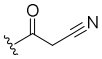	243	1143 [5]	1542 [6]	ND[e] -
23		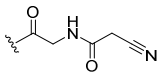	95	69 [1]	89 [1]	ND[e] -
24	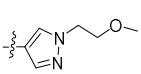	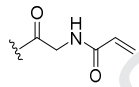	66	1542 [23]	56 [1]	ND[e] -
25	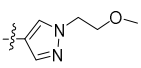	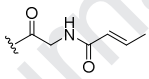	108	886 [9]	45 [0.4]	ND[e] -
26	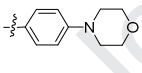	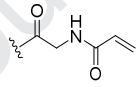	103	>3000 -	354 [3]	ND[e] -
27	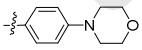	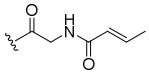	375	ND[e] -	586 [2]	ND[e] -
28	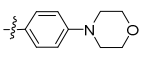	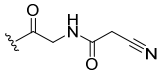	253	309 [1]	1432 [6]	ND[e] -
29	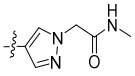	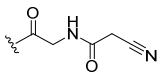	127	2732 [22]	>3000 -	ND[e] -
30	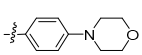		33	2788 [85]	ND[e] -	2653 [577]
31	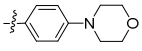	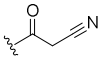	152	216 [1]	2233 [15]	>3000 -
32	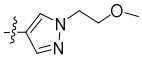		76	ND[e] -	2764 [36]	ND[e] -
33	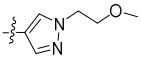	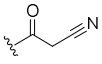	86	1459 [17]	2677 [31]	1872 [22]
34			99	2155 [22]	321 [3]	ND[e] -

35	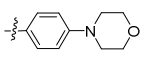	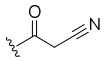	78	ND[e] -	528 [7]	ND[e] -
36	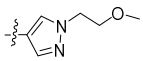	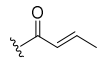	14	1981 [142]	1445 [103]	>3000 -
37	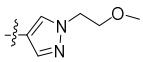	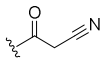	24	ND[e] -	183 [8]	2496 [104]
38	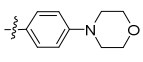	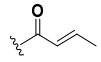	**6.1**	1412 **[232]**	1147 **[188]**	>3000 -
39	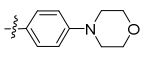	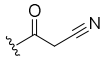	15	88 [6]	433 [29]	>3000 -
Tofacitinb			0.9	1.5 [1.7]	1.3 [1.4]	35.5 [39.4]

[a] IC_{50} values are the average of duplicate experiments.

[b] Fold selectivity derived from JAK2/JAK3 enzyme IC_{50}.

[c] Fold selectivity derived from JAK1/JAK3 enzyme IC_{50}.

[d] Fold selectivity derived from TYK2/JAK3 enzyme IC_{50}.

[e] ND = not determined.

N-methyl-6-(3-(substituted amino)phenyl)pyrimidin-4-amine derivatives (**1-6**, **13-29**) were synthesized with changes in the side chain (R_1) and tail (R_2). Several analogs using different ammonia groups (Table 2) were generated to develop stronger JAK3 inhibitors, including compounds **1-6** that showed an IC_{50} of 100-600 nM against JAK3. Next, to improve potency for JAK3, the SAR of the tail (R_2) for compounds **13-29** was investigated (Table 3). When butenamide groups were introduced (compounds **15** and **17**), both the inhibitory activities and selectivity for JAK3 increased up to 3-6-fold, when compared with compounds **2** and **3**. The resulting increase in inhibitory activities might be attributed to the length of the tail that covalently reacts with Cys909 in JAK3 kinases. Nevertheless, when the "length" of amide in compounds **15** and **17** was enhanced, creating compounds **23-29**, a decrease in inhibitory activities against JAK3 was observed. Therefore, *para*-substituted compounds **9-10** and **32-35** at the 4-position of the phenyl ring were designed for further modifications. The results showed that compounds showed a significant increase in inhibitory activities against JAK3.

Replacement of 4,6-substituted pyrimidine with 2,4-substituted pyrimidine (compounds **7-8**, **11-12**, **30-31**, and **36-39**, Table 2 and 3) retained the activities against JAK3 (inhibitory potency with an IC_{50} ranging between 1.7 nM to 55 nM) and

selectivity for JAK3 versus other kinases. Among this series, regarding the feature of the hydrophobic cavity, we mainly explored the side chain is 1-(2-methoxyethyl)-1*H*-pyrazol-4-amine or 4-morpholinoaniline. Compound **12** exhibited excellent inhibitory activity against JAK3 (IC_{50} = 1.7 nM) and unprecedented selectivity (777-fold JAK1/3 and 588-fold JAK2/3), when compared to other derivatives. The results revealed that 4-morpholinoaniline (compounds **12** and **38**) have a higher potency compared to a pyrazole ring (**11** and **36**) at the 2-position of the pyrimidine ring. Compounds **12** (*C*log*P* = 3.77) and **38** (*C*log*P* = 4.02) exhibited a higher lipophilicity compared to compounds **11** and **36** (Table 4), respectively. The results demonstrated that the hydrophobic aromatic amine group improved the JAK3 inhibitory activity, which can be confirmed by molecular docking study where the hydrophobic aromatic amine group can create two σ-π interactions with amino acids Leu828 and Gly908 (Fig. 3). After comparing the above-mentioned derivatives, we concluded that compounds with a *para*-acrylamide on the phenyl ring showed the greatest potency against JAK3 among others with *meta*-acrylamide. A similar trend was observed among other analogues with their parent compounds in 4,6-substituted pyrimidine derivatives. Based on the above-mentioned SAR, compounds **11**, **12**, and **38** were selected as tool compounds for additional studies.

2.3. Molecular docking study

Based on the above discussion, compound **12** possessed the best inhibitory activities and selectivity for JAK3. To investigate the possible binding mode of compound **12** with JAK3 (PDB: 4Z16), computer simulation of molecular docking is performed by Molecular Operating Environment (MOE) software. As shown in Fig. 3, the anilinopyrimidine moiety of compound **12** makes the expected bidentate hinge hydrogen bonds with Leu905, and continuous electron density was observed between the acrylamide warhead and Cys909, indicative of covalent bond formation. The major difference in JAK3 binding models is that two σ-π interactions are produced by the morpholinoaniline of **12** with the amino acids Leu828 and Gly908 and a σ-π interaction between the pyrimidine core of **12** with the amino acid Leu828.

Presumably, these interactions enhanced the activity of **12** against JAK3. Interestingly, the thiol group and Asp912 formed a hydrogen bond after the acryl group of compound **12** and the thiol group of residue Cys909 form a covalent bond, which indicated that compound **12** had tight contact with the ATP-binding pocket in JAK3. These docking observations reasonably explain the activity data.

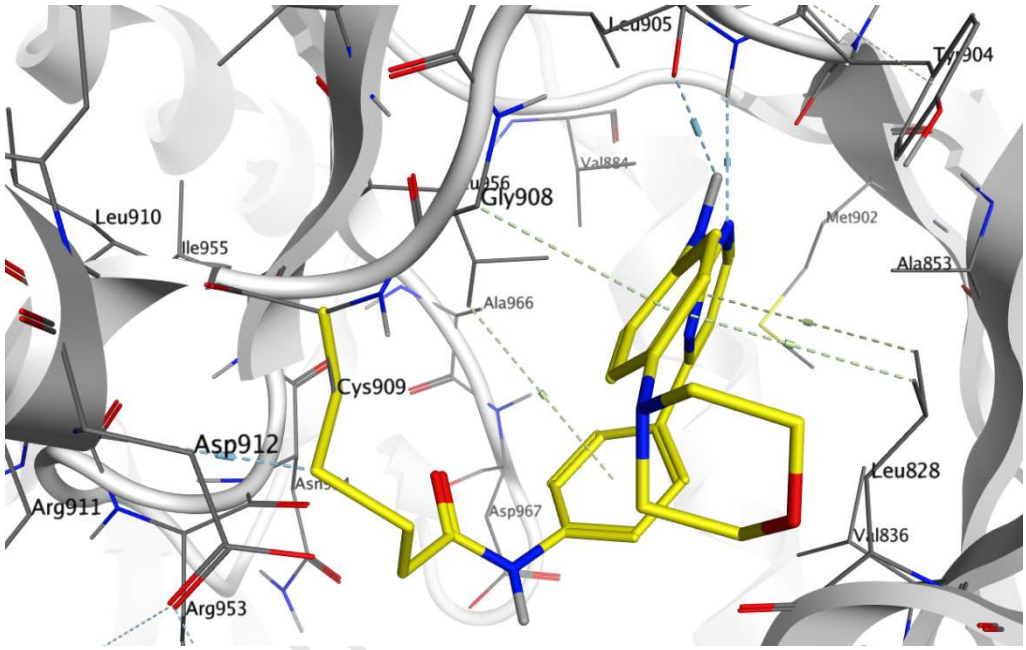

Fig. 3. Compound **12** bound to JAK3 enzyme (PDB code: 4Z16). 3D interaction diagram representing the docked conformation of compound **12** covalently binds to Cys909 of JAK3 enzyme.

2.4. Cell cytotoxicity evaluation

To evaluate the effects of active compounds **11**, **12**, and **38** on the cell viability, resting mouse T cells, IL-4-treated activated T cells, and Raw 264.7 cells were used for the CellTiter 96® AQueous One Solution Cell Proliferation Assay (MTS assay). In general, resting T cells and IL-4-treated activated T cells do not have the ability to proliferate, but maintain normal survival. Raw 267.4 cells served as non-lymphocyte controls, and were selected for cytotoxicity evaluation. Treatment of the three cell types with compounds **11**, **12**, and **38** for 72 h at 10 μM, showed that three compounds did not have any influence on the three cell types (Fig. 4). Taken together,

these results indicated that the compounds had no obvious cytotoxicity against these cells when used at a concentration of 10 μM.

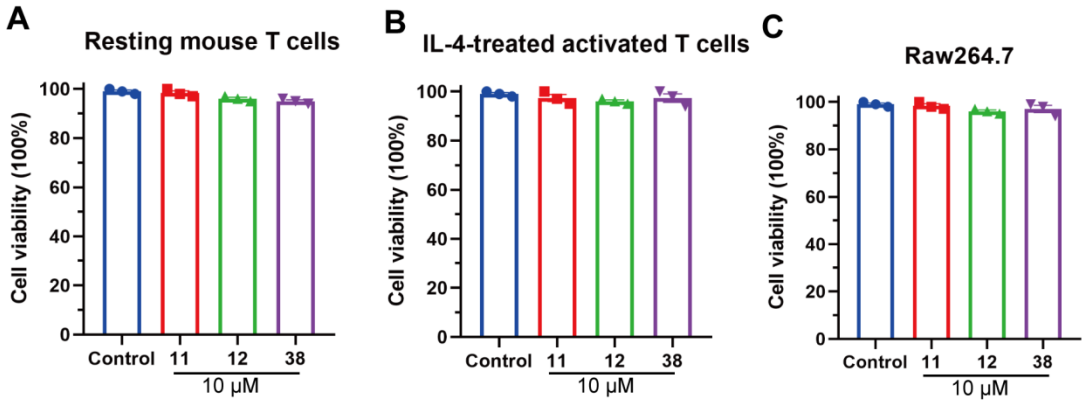

Fig. 4. The cell viability of **11**, **12**, and **38** was determined by the MTS method. Resting mouse T cell (A), IL-4-treated activated T cell (B), and RAW264.7 cells (C) were respectively treated with compounds **11**, **12**, and **38** at 10 μM for 72 h, and cytotoxicity was expressed by the percentage of surviving cells over control cells.

2.5. Compounds on T cell proliferation in vitro

Based on the inhibitory potency and selectivity of compounds for JAK3, compounds **11**, **12**, and **38** were selected for further evaluation. In addition, their anti-proliferative activity against mouse T cell lines was assessed using the MTS assay. To analyze the immunosuppressive activity, mouse T cells were purified and activated with or without anti-CD3/-CD28 or IL-2 in the presence or absence of different concentrations of compounds **11**, **12**, and **38** for 72 h, then, the proliferation of T cells was analyzed by the MTS assay. As shown in Table 4, compounds **11**, **12**, and **38** significantly suppressed T cell proliferation when stimulated by anti-CD3/CD28 with IC_{50} values of 6.49, 0.83, and 1.60 μM or IL-2 with IC_{50} value of 7.5, 0.77, and 2.11 μM, respectively. Especially, compound **12** displayed a stronger inhibition for T cell proliferation when compared to tofacitinib with an IC_{50} value of 0.83 vs 1.38 (anti-CD3/CD28 stimulation) and 0.77 vs 1.54 (IL-2 stimulation),

respectively. Together, our data demonstrated that compound **12** showed obvious significant immunosuppressive activity under selective inhibition of JAK3.

Table 4.
The effects of compounds inhibiting T cell proliferation after stimulation by anti-CD3/-CD28 or IL-2.

Compound	Inhibition of T cell proliferation, IC_{50}(μM)		*C*log*P* [a]
	anti-CD3/-CD28	IL-2	
11	6.49	7.50	2.18
12	**0.83**	**0.77**	3.77
38	**1.60**	**2.11**	4.02
Tofacitinib	1.38	1.50	1.54

[a] *Calculated as miLogP using Molinspiration property engine version 2018.10 (http://www.molinspiration.com).*

*2.6. Compound **12** selectively inhibits JAK3-dependent signaling in live cells*

To test whether the compounds were effective in a native cellular environment, we evaluated the ability of compounds to inhibit STAT5 phosphorylation in live cells using tofacitinib as a control. As shown in Fig. 5, IL-2 or IL-15-induced STAT5 phosphorylation was significantly inhibited when used at a concentration of 10 μM after incubating mouse T cells with compounds **11**, **12**, and **38** for 1 h (Fig. 5A, B). Compared to the other two compounds and tofacitinib, compound **12** exhibited better inhibitory activity when used at the same concentration (10 μM). Further analysis indicated that compound **12** almost completely abrogated IL-2 or IL-15-induced phosphorylation of STAT5 at 1 μM treatment in a concentration-dependent manner (Fig. 5C, D). Data obtained from the cellular signaling pathway level further confirmed the selective activity of compound **12** on JAK3. Thus, these results demonstrated that compound **12** had potent inhibitory activity and selectivity on JAK3.

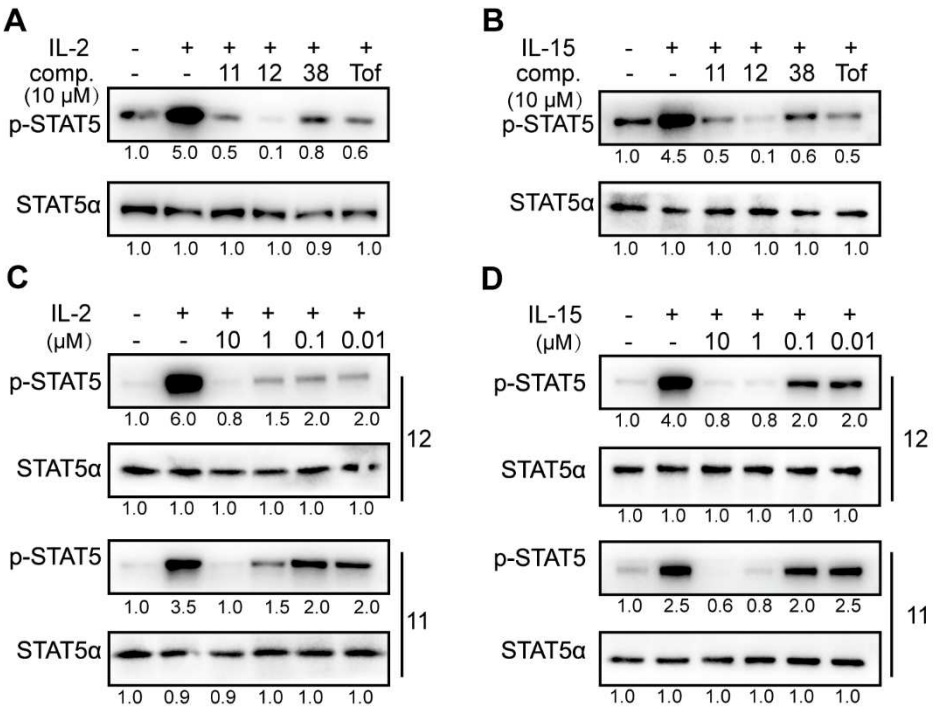

Fig. 5. Compounds potently and selectively inhibited JAK3-dependent signaling in mouse T cells. After pre-incubating with compounds **11**, **12**, and **38** for 2 h at 10 μM, T cells were stimulated with IL-2 (A) or IL-15 (B) for another 30 min. The levels of p-STAT5 were determined by Western blot analysis. The concentration-dependent expression of p-STAT5 was further determined by indicated concentrations of compounds **11** and **12** for 2 h prior to IL-2 (C) or IL-15(D) stimulation to T cells. Tof (tofacitinib) served as a positive agent in this assay.

*2.7. Kinase selectivity profiling of compound **12***

To further understand the selective kinase profile, the inhibitory effect of compound **12** for tyrosine kinases other than JAK family isoforms were evaluated, including BLK, BMX, BTK, EGFR, ERBB2, ERBB4, ITK, RLK, and TEC, which all carry a thiol in a position analogous to that of Cys909 in JAK3. The results are presented in Table 5, and show that compound **12** exhibited a potent inhibition rate of 100% for JAK3 at a concentration of 100 nM. However, the inhibition rate of the other 9 kinases was much lower than that of JAK3. Taken together, our data indicated that compound **12** exhibited a higher selective inhibition to JAK3 than other kinases with a cysteine at a position compared to that of Cys909.

Table 5.
The inhibitory activity of compound **12** (100 nM) on other kinases.

compd	Inhibition rate (%)									
	JAK3	**BLK**	**BMK**	**BTK**	**EGFR (ErbB1)**	**ERBB2 (HER2)**	**ERBB4 (HER4)**	**ITK**	**RLK**	**TEC**
12	100	20.6	3.7	6.3	1.2	19.2	8.0	2.3	2.9	29.5

Biochemical assays were conducted using SelectScreen® Kinase Profiling by Z'-LYTE (TEC by Lantha Screen) at the Km concentration of ATP.

*2.8. Compound **12** covalently binds to JAK3 and irreversibly inhibits JAK3*

To confirm that compound **12** irreversibly interacted with JAK3, a time-dependent inhibition assay was performed (Fig. 6A). For fair comparison, the concentration was performed at 2 nM at which compounds were profiled reflects their JAK3 potency. Extending the pre-treatment time of compound **12** with JAK3 improved the inhibitory effect, whereas the reversible inhibitor tofacitinib did not exhibit such time-dependent behavior (Fig. 6A). To further determine if compound **12** shared the features of irreversible inhibitors, the dissociation kinetics of compound **12** were evaluated. Compound **12** at an IC_{90} (500 nM) was mixed and incubated with JAK3 for 30 minutes to allow complete association. This mixture was then diluted with kinase buffer 1000-fold to less than the IC_{10}, and the enzymatic activity was evaluated via measuring the phosphorylated product by TR-FRET. The recovery rate of kinase activity related to JAK3 that had not been exposed to compound **12** was measured. Pre-treatment of JAK3 with compound **12** resulted in lack of any measurable JAK3 activity once the compound was diluted, suggesting that the inhibitor irreversibly bound to JAK3 for more than 24 hours (Fig. 6B).

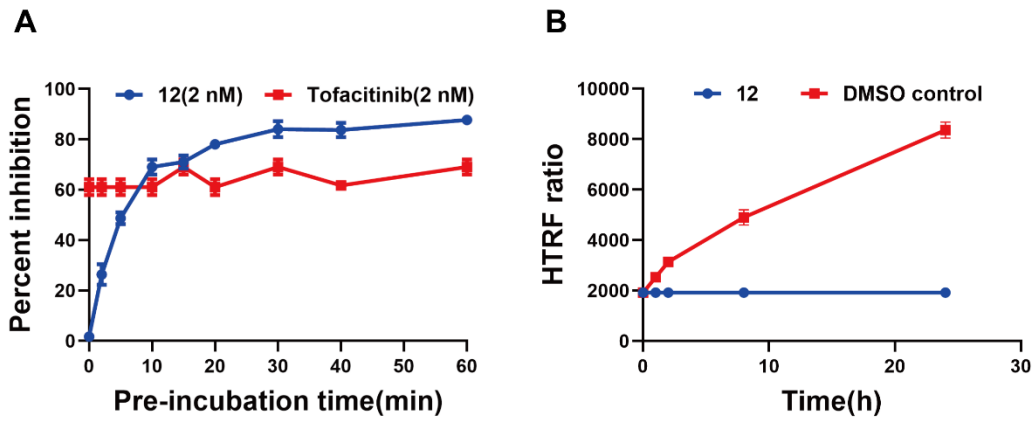

Fig. 6. (A) Time-dependent inhibition curves of compound **12** and Tofacitinib. (B) JAK3 enzymatic activity was not restored up to 24 hours after diluting from an IC_{90} to an IC_{10} concentration of compound **12** (blue) when compared to a DMSO control (red).

2.9. Pharmacokinetic property evaluation

Preliminary pharmacokinetic (PK) properties of compound **12** were performed in male ICR (Institute of Cancer Research) mice following intravenous and oral administration. The results are summarized in Table 6 and the corresponding concentration-time curve was showed in Fig. S1 of supplementary material. Upon oral administration of 30 mg/kg, compound **12**, a reasonable PK profile was obtained with a $t_{1/2}$ of 1.52 h, area under curve (AUC) of 889.42 μg/L*h, and moderate bioavailability of 23.82%. These data suggested that compound **12** may be a useful probe for cellular and animal studies.

Table 6.
Preliminary pharmacokinetic data of compound **12** in male ICR Mice.

Compound 12	iv (10 mg/kg)	po (30 mg/kg)
AUC(0-t) (μg/L*h) [a]	1244.41±77.83	889.42±48.32
AUC(0-∞) (μg/L*h)	1274.41±57.18	897.12±56.72
MRT (0-∞)(h) [b]	0.73±0.08	1.42±0.38
Vz (L/kg) [c]	8.36±1.83	220.42±24.71
CLz (L/h/kg) [d]	8.15±1.21	97.14±20.87
$t_{1/2}$ (h) [e]	0.47±0.06	1.52±0.34
C_{max} (μg/L) [f]	8763.23±324.65	2008.21±189.44

Bioavailability(%) [g]	23.82%

[a] Area under the concentration time curve. [b] Mean residence time

[c] Volume in steady state. [d] Plasma clearance. [e] Terminal half-life.

[f] Peak plasma concentrations. [g] Bioavailability = AUC_{0-t}(po)/AUC_{0-t}(iv) × 100%

2.10. In vivo immunosuppressive activity

*2.10.1. Compound **12** inhibited oxazolone-induced delayed type hypersensitivity reaction*

Delayed type hypersensitivity (DTH) reaction is a T cell-mediated pathologic response. To test the immunosuppressive activity of compounds **11**, **12**, and **38** *in vivo*, the effects of these compounds on an oxazolone (OXZ)-induced DTH Balb/c mice model [30] were determined using tofacitinib as the positive control [31] (Fig. 7A). Following sensitization by OXZ, mice were administrated compounds or tofacitinib by p.o. at a dose of 30 mg/kg. Ear swelling and spleen index were used to assess the effect of drugs. Following 7 days of administration, only compound **12** displayed a significant reduction of ear swelling by OXZ-induced DTH (Fig. 7B, C). In addition, all agents showed a reduction in the spleen index, and compound **12** and tofacitinib exhibited potent suppression (Fig. 7D). The spleen index is an important index to evaluate immunosuppression, and our data indicated that compound **12** exhibited obvious immunosuppressive activity.

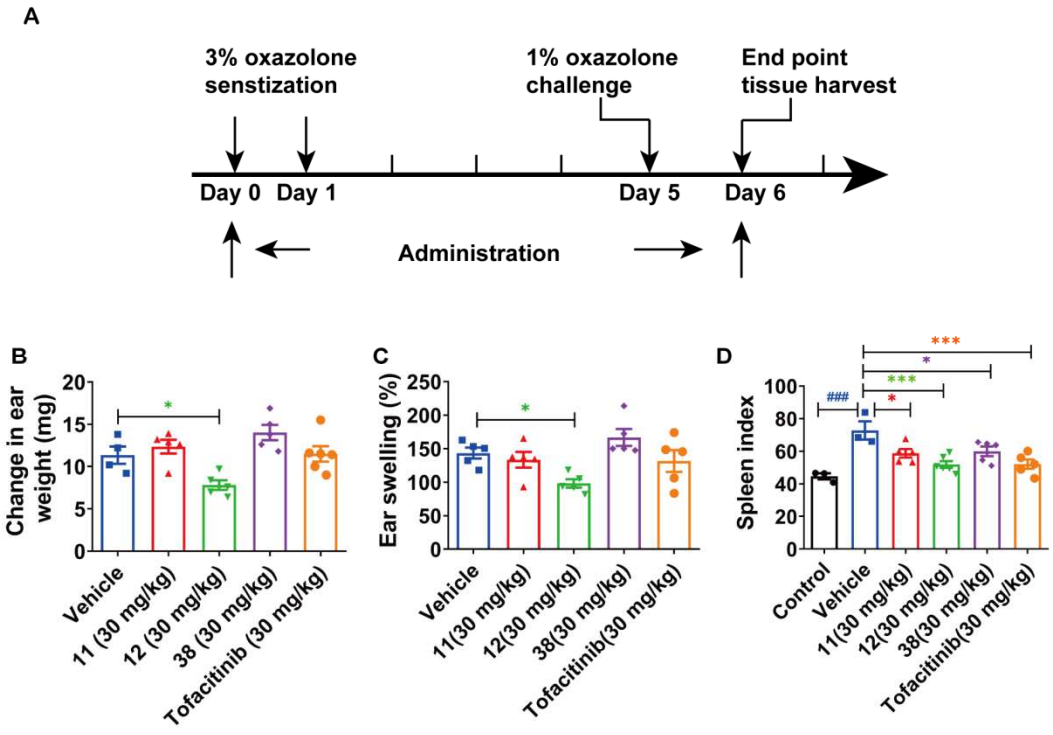

Fig. 7. The effect of compounds **11**, **12**, and **38** on oxazolone (OXZ)-induced delayed type hypersensitivity (DTH) mouse model. (A) Timeline for the process of DTH development and treatment. Ear weight (B), the percentage of ear swelling (C), and the spleen index (D) were presented to evaluate the effect of compounds **11**, **12**, and **38** on OXZ-induced DTH responses. Tofacitinib served as a positive agent for compounds. Data are presented as the mean ± SEM. n = 5-6 per group for treated mice and 3 for control mice. $^{\#\#\#}p < 0.001$ versus control group; $^{*}p < 0.05$, $^{**}p < 0.01$, and $^{***}p < 0.001$ versus vehicle group.

*2.10.2. Compound **12** inhibited dose-dependent OXZ-induced DTH responses*

To further evaluate the effect of compound **12** on OXZ-induced DTH responses, three doses of compound **12** were administered to OXZ-induced DTH mice. Our results indicated that in OXZ-induced DTH mice, compound **12** reduced edema of ear tissue in a dose-dependent manner (Fig. 8A, B). In addition, high doses of compound **12** and tofacitinib significantly inhibited the spleen index (Fig. 8C). Histopathological changes and inflammatory cell infiltration were evaluated by eosin and hematoxylin (HE) staining. HE-staining showed less neutrophil leukocyte infiltration and

well-structured tissue architecture in the mice that were given compound **12** (30 mg/kg) when compared to the vehicle group (Fig. 8D), which showed significant dense neutrophil leukocyte infiltration and increased ear thickness. Upon oral administration of 30 mg/kg compound **12**, the neutrophil leukocyte infiltration was reduced and edema was decreased, and ear tissue was similar to that in control tissues.

In addition, no signs of toxicity were observed in compound-treated mice based on body weight and microscopic examination of individual organs (data not shown).

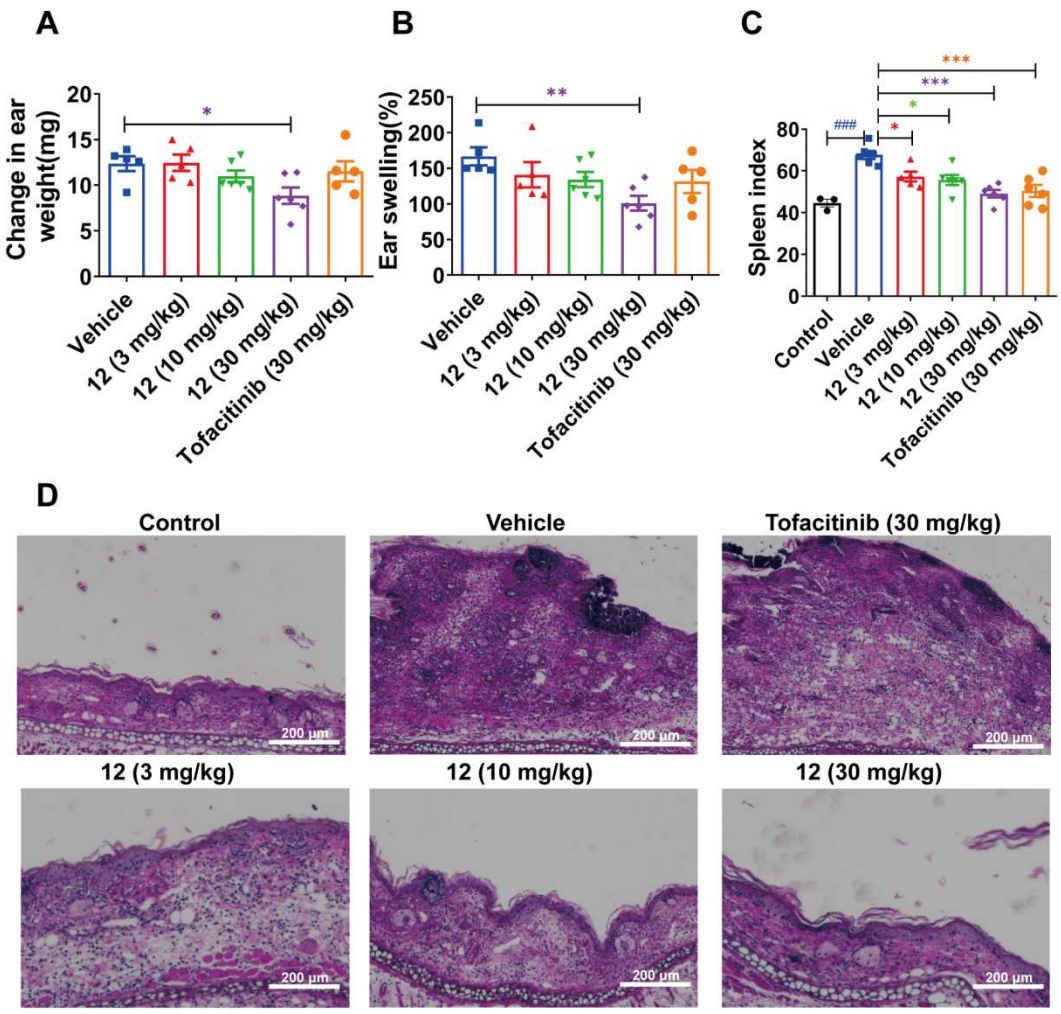

Fig. 8. Immunosuppressive effects of compound **12** on oxazolone-induced delayed type hypersensitivity mice. (A-C) Compound **12** (30, 10, and 3 mg/kg, p.o.) inhibited oxazolone (OXZ)-induced delayed type hypersensitivity (DTH) responses in a dose-dependent manner. (D) The effect of compound **12** on histopathological changes

and inflammatory cell infiltration were evaluated by HE-staining in ear tissue. Scale bar 200 μm. Tofacitinib was positive agent and compared with compound **12**. Data are the mean ± SEM. n = 5-6 per group for treated mice and 3 for control mice. $^{###}p < 0.001$ versus control group; $^{*}p < 0.05$, $^{**}p < 0.01$, and $^{***}p < 0.001$ versus vehicle group.

3. Conclusion

JAK is a confirmed pivotal target for immune and inflammatory diseases, and there is continuous interest in the discovery of novel selective inhibitors that overcome the side effects. In a recent study, novel derivatives were designed and synthesized based on 4- or 6-phenyl-pyrimidine as novel selective JAK3 inhibitors. After primary SAR analysis and enzymatic inhibitory activity *in vitro*, compound **12** showed a highly potent and selective inhibition for JAK3 with an IC_{50} value of 1.7 nM, and exceeding 588-fold selectivity versus other enzymes in the JAK family. Molecular docking studies suggested that compound **12** might covalently bind to the Cys909 position of JAK3. T cell proliferation and kinase signal pathway experiments revealed that compound **12** presented a high selectivity within the JAK family. Further *in vivo* studies using an OXZ-induced DTH mouse model indicated that compound **12** had significant anti-inflammatory and immunosuppressive activities. Moreover, compound **12** possessed reasonable oral pharmacokinetic properties. Therefore, the data obtained in the current study suggested that compound **12** may be a promising tool compound for treating autoimmune diseases as a selective JAK3 inhibitor.

4. Experimental procedures

4.1. Chemistry and chemical methods

Unless specified otherwise, all starting materials, reagents, and solvents were commercially available and used without further purification. All chemicals or reagents were of analytical grade. Silica gel (200–300 mesh, Qingdao city, China) was used for column chromatography. The progress of reactions was monitored by analytical thin-layer chromatography (TLC) on silica gel plates (GF-254) and

visualized under UV light at 254 or 365 nm. Melting points of individual compounds were determined using a Mel-TEMP II and melting point apparatus uncorrected. ^{1}H NMR and ^{13}C NMR spectra were recorded using a Bruker ARX-300 spectrometer with TMS as the internal standard in $CDCl_3$, DMSO-*d*6. Peak multiplicities were abbreviated as follows: singlet, s; doublet, d; triplet, t; m, multiplet; dd, double doublet. Mass spectrum (MS) was obtained on an Agilent 6120 quadrupole LC/MS (ESI). High resolution mass spectrum (HRMS) was run on an Agilent Q-TOF mass spectrometer.

*4.1.1 4-Chloro-6-(3-nitrophenyl)pyrimidine (**40**)*

3-Bromonitrobenzene (1 g, 5.0 mmol), bis(pinacolato)diboron (1.34 g, 2.6 mmol), KOAc (1.48 g, 7.5 mmol), and $Pd(PPh_3)_4$ (0.11 g, 0.09 mmol) were combined in 1,4-dioxane (50 mL). The reaction mixture was placed into an oil bath preheated to 100 □, with stirring at this temperature for 12 h under argon. When completion of the reaction showed TLC, cooled to room temperature, respectively added to 2,6-dichloropyrimidine (1.07 g, 7.2 mmol), 2M K_2CO_3 (2 g, 14.5 mmol) aqueous solution and $Pd(PPh_3)_4$ (0.10 g, 0.09 mmol), heated to 100 °C in oil bath, stirred at this temperature for 12 h under argon. The reaction mixture was filtered through a Celite bed, and the filtrate was concentrated and purified by silica gel column chromatography (hexane: ethyl acetate = 50:1) to afford **40** as a white solid (0.82 g, total yield 68%). ^{1}H NMR (300 MHz, $CDCl_3$) δ 9.11 (s, 1H), 8.95 (s, 1H), 8.45 (d, *J* = 8.0 Hz, 1H), 8.41 (d, *J* = 9.3 Hz, 1H), 7.85 (s, 1H), 7.74 (t, *J* = 8.0 Hz, 1H).

*4.1.2. 4-Chloro-6-(4-nitrophenyl)pyrimidine (**43**)*

Compound **43** was prepared with the same procedures as for **40** as reported in 70% total yield. ^{1}H NMR (300 MHz, $CDCl_3$) δ 9.11 (s, 1H), 8.38 (d, *J* = 8.8 Hz, 2H), 8.27 (d, *J* = 8.8 Hz, 2H), 7.83 (s, 1H).

*4.1.3. 2-Chloro-4-(3-nitrophenyl)pyrimidine (**46**)*

Compound **46** was prepared with the same procedures as for **40** as reported in 81% total yield. ^{1}H NMR (300 MHz, $CDCl_3$) δ 8.92 (s, 1H), 8.76 (d, *J* = 5.2 Hz, 1H), 8.48 (d, *J* = 7.9 Hz, 1H), 8.40 (d, *J* = 7.1 Hz, 1H), 7.76 – 7.73 (m, 2H).

*4.1.4. 2-Chloro-4-(4-nitrophenyl)pyrimidine (**49**)*

Compound **49** was prepared with the same procedures as for **40** as reported in 76% total yield. ^{1}H NMR (300 MHz, $CDCl_3$) δ 8.76 (d, *J* = 5.2 Hz, 1H), 8.37 (d, *J* = 8.9 Hz, 2H), 8.28 (d, *J* = 8.9 Hz, 2H), 7.73 (d, *J* = 5.2 Hz, 1H).

*4.1.5. N-(1-methyl-1H-pyrazol-4-yl)-4-(3-nitrophenyl)pyrimidin-2-amine (**41a**)*

To **40** (0.2 g, 0.85 mmol) and 1-methyl-1*H*-pyrazol-4-amine hydrochloride salt (0.13 g, 0.94 mmol) in isopropyl alcohol (8 mL) was added *N*,*N*-diisopropylethylamine (DIEA, 0.27g, 2.13 mmol), and the mixture was stirred overnight at 110°C. The mixture was then concentrated, and purified by column chromatography (DCM: MeOH = 40:1) to yield 0.21 g (82%) of **41a** as a light yellow solid. ^{1}H NMR (300 MHz, DMSO) δ 8.82 (s, 1H), 8.71 (s, 1H), 8.44 (d, *J* = 7.8 Hz, 1H), 8.35 (d, *J* = 8.2 Hz, 1H), 8.04 (s, 1H), 7.82 (t, *J* = 7.9 Hz, 1H), 7.54 (s, 1H), 7.21 (s, 1H), 3.84 (s, 3H).

Compounds **41b-f**, **44b-c**, **47b-c**, and **50b-c** were prepared following the similar synthetic procedure of compound **41a**. Detailed experimental procedure and spectral data are presented in the supplementary material.

*4.1.6. 4-(3-Aminophenyl)-N-(1-methyl-1H-pyrazol-4-yl)pyrimidin-2-amine (**42a**)*

To **41a** (0.28g, 0.95 mmol) and 10% Pd/C 0.1g in EtOH (50 mL) was added drop by drop 85% hydrazine hydrate (0.47 g, 9.5 mmol) at 88 °C. The reaction mixture was stirred for 2h under nitrogen. The mixture was then filtered with a Celite bed, the filtrate was concentrated and dried under vacuum to yield 0.24 mg (95%) of **42a** as a white solid. ^{1}H NMR (300 MHz, DMSO) δ 8.60 (s, 1H), 8.00 (s, 1H), 7.50 (s, 1H), 7.26 (s, 1H), 7.12 (s, 2H), 6.97 (s, 1H), 6.80 – 6.56 (m, 1H), 3.83 (s, 3H).

Compounds **42b-f**, **45b-c**, **48b-c**, and **51b-c** were prepared following the similar synthetic procedure of compound **42a**. Detailed spectral data are presented in the supplementary material.

*4.1.7. Tert-butyl(2-((3-(2-((1-methyl-1H-pyrazol-4-yl)amino)pyrimidin-4-yl)phenyl) amino)-2-oxoethyl)carbamate (**52a**)*

To a solution of *N*-((2,2-dimethylpropoxy)carbonyl)-glycine (0.2 g, 1.13 mmol) in DCM (10 mL), 1-(3-dimethylaminopropyl)-3-ethylcarbodiimide hydrochloride (EDCI, 0.36 g, 1.88 mmol), 1-hydroxybenzotriazole (HOBT, 0.25 g, 1.88 mmol), and DIEA (0.34 g, 2.6 mmol) were added, respectively. And the mixture was stirred for 30min at 0□. **42a** (0.2 g, 0.75 mmol) was added to the reaction mixture, then allowed to warm to room temperature with stirring for 6h. After completion of the reaction, the mixture was extracted with DCM, washed with brine, and the organic phase was dried over Na_2SO_4. The solvent was removed and the residue was purified by flash column chromatography on silica (DCM: MeOH = 30:1) to give a yellow solid (0.27g, 85%). ^{1}H NMR (300 MHz, $CDCl_3$) δ 8.64 (s, 1H), 8.00 (s, 1H), 7.76 (s, 1H), 7.60 (s, 1H), 7.58 (s, 1H), 7.55 (s, 1H), 7.34 – 7.27 (m, 1H), 6.77 (s, 1H), 3.98 (d, *J* = 5.6 Hz, 2H), 3.90 (s, 3H), 1.46 (s, 9H).

Compounds **52b-c** and **52e** were prepared following the similar synthetic procedure of compound **52a**. Detailed spectral data are presented in the supplementary material.

*4.1.8. 2-Amino-N-(3-(2-((1-methyl-1H-pyrazol-4-yl)amino)pyrimidin-4-yl)phenyl) acetamide (**53a**)*

To a solution containing **52a** (0.5 g, 1.34 mmol) in 2 mL of dry DCM, cooled to 0 °C was slowly added TFA (2 mL, 13 mmol). After the consumption of the starting material (5 h, monitored by TLC), the solvent was evaporated, and removed under vacuum. Semi-solid was slurred with dry ether, and filtered to afford crude product (0.36 g, 98%), which was used directly in the next step.

Compounds **53b-c** and **53e** were prepared following the similar synthetic procedure of compound **53a**. Detailed spectral data are presented in the supplementary material.

Method A: General procedure for the synthesis of targets **1-12**, **13**, **15**, **17**, **19-21**, **24-27**, **30**, **32**, **34**, **36**, and **38**.

To a solution of **42a** (0.1 g, 0.37 mmol) in THF (5 mL) were added DIEA (0.05g, 0.37 mmol) and acryloyl chloride (0.03g, 0.37 mmol) at -5 °C. The resulting mixture was stirred for 30 min. Then it was quenched by MeOH (2 mL), concentrated, and purified by silica gel column chromatography (DCM: MeOH = 20:1) to afford the title compounds.

*4.1.9. N-(3-(6-((1-methyl-1H-pyrazol-4-yl)amino)pyrimidin-4-yl)phenyl)acrylamide (**1**)*

White solid (yield: 71%). m. p.: 214–216 □. ^{1}H NMR (300 MHz, DMSO) δ 8.65 (s, 1H), 8.44 (s, 1H), 8.01 (s, 1H), 7.79 (d, *J* = 7.9 Hz, 1H), 7.71 (d, *J* = 7.8 Hz, 1H), 7.52 (s, 1H), 7.46 (t, *J* = 7.9 Hz, 1H), 7.07 (s, 1H), 6.47 (dd, *J* = 16.9, 10.0 Hz, 1H), 6.32 – 6.26 (m, 1H), 5.80 – 5.75 (m, 1H), 3.84 (s, 3H); ^{13}C NMR (75 MHz, DMSO) δ 163.35, 160.38, 158.48, 139.52, 137.60, 131.79, 130.66, 129.26, 127.01, 122.03, 121.44, 120.96, 117.41, 104.10, 100.75, 38.72; HRMS *m/z* (ESI): calcd for $C_{17}H_{17}N_6O$ $[M+H]^+$ 321.1461, found 321.1460.

*4.1.10. N-(3-(6-((1-(2-methoxyethyl)-1H-pyrazol-4-yl)amino)pyrimidin-4-yl)phenyl) acrylamide (**2**)*

White solid (yield: 72%). m. p.: 213–215 □. 213.2–215.1□. ^{1}H NMR (300 MHz, DMSO) δ 8.69 (s, 1H), 8.48 (s, 1H), 8.06 (s, 1H), 7.81 (d, *J* = 7.7 Hz, 1H), 7.73 (d, *J* = 7.5 Hz, 1H), 7.59 (s, 1H), 7.47 (t, *J* = 7.8 Hz, 1H), 7.10 (s, 1H), 6.49 (dd, *J* = 16.9, 10.0 Hz, 1H), 6.31 (d, *J* = 16.7 Hz, 1H), 5.78 (d, *J* = 10.6 Hz, 1H), 4.25 (t, *J* = 4.9 Hz, 2H), 3.68 (t, *J* = 4.9 Hz, 2H), 3.23 (s, 3H); ^{13}C NMR (75 MHz, DMSO) δ 163.31, 160.23, 158.52, 139.54, 137.56, 131.77, 130.61, 129.26, 127.03, 121.88, 121.38, 120.91, 117.34, 101.03, 70.65, 57.92, 51.33; HRMS *m/z* (ESI): calcd for $C_{19}H_{21}N_6O_2$ $[M+H]^+$ 365.1882, found 365.1880.

*4.1.11. N-(3-(6-((4-morpholinophenyl)amino)pyrimidin-4-yl)phenyl)acrylamide (**3**)*

White solid (yield: 74%). m. p.: 224–225 □. 223.7–225.1□. ^{1}H NMR (300 MHz, DMSO) δ 8.62 (s, 1H), 8.45 (s, 1H), 7.80 (d, *J* = 7.3 Hz, 1H), 7.69 (d, *J* = 7.0 Hz, 1H), 7.53 (d, *J* = 8.2 Hz, 2H), 7.46 (t, *J* = 7.8 Hz, 1H), 7.15 (s, 1H), 6.95 (d, *J* = 8.8 Hz, 2H), 6.50 (dd, *J* = 16.6, 10.2 Hz, 1H), 6.29 (d, *J* = 17.0 Hz, 1H), 5.78 (d, *J* = 10.1 Hz, 1H), 3.74 (s, 4H), 3.06 (s, 4H); ^{13}C NMR (75 MHz, DMSO) δ 163.82, 161.63, 161.06, 158.77, 147.52, 140.04, 138.10, 132.27, 129.75, 127.48, 122.07, 121.85, 121.43, 117.80, 116.14, 101.63, 66.60, 49.04; HRMS *m/z* (ESI): calcd for $C_{23}H_{24}N_5O_2$ $[M+H]^+$ 402.1926, found 402.1924.

*4.1.12. N-(3-(6-((1-(2-(dimethylamino)ethyl)-1H-pyrazol-4-yl)amino)pyrimidin-4-yl) phenyl)acrylamide (**4**)*

White solid (yield: 65%). m. p.: 198–199 □. ^{1}H NMR (300 MHz, DMSO) δ 8.66 (s, 1H), 8.47 (s, 1H), 8.06 (s, 1H), 7.80 (d, *J* = 6.4 Hz, 1H), 7.71 (d, *J* = 7.2 Hz, 1H), 7.55 (s, 1H), 7.47 (t, *J* = 7.5 Hz, 1H), 7.09 (s, 1H), 6.49 (dd, *J* = 16.7, 10.0 Hz, 1H), 6.30 (d, *J* = 17.1 Hz, 1H), 5.78 (d, *J* = 10.0 Hz, 1H), 4.18 (s, 2H), 2.63 (t, *J* = 5.7 Hz, 2H), 2.16 (s, 6H); ^{13}C NMR (75 MHz, DMSO) δ 163.27, 160.01, 158.51, 149.03, 139.56, 137.54, 131.79, 129.27, 127.02, 121.32, 120.86, 117.27, 101.01, 58.71, 49.61, 45.11; HRMS *m/z* (ESI): calcd for $C_{20}H_{24}N_7O$ $[M+H]^+$ 378.2044, found 378.2041.

*4.1.13. N-(3-(6-((1-(2-(methylamino)-2-oxoethyl)-1H-pyrazol-4-yl)amino)pyrimidin-4-yl)phenyl)acrylamide (**5**)*

White solid (yield: 66%). m. p.: 244–245 □. ^{1}H NMR (300 MHz, DMSO) δ 8.68 (s, 1H), 8.47 (s, 1H), 8.09 (s, 1H), 7.81 (d, *J* = 3.5 Hz, 1H), 7.72 (d, *J* = 7.0 Hz, 1H), 7.58 (s, 1H), 7.47 (t, *J* = 7.8 Hz, 1H), 7.11 (s, 1H), 6.50 (dd, *J* = 16.4, 9.7 Hz, 1H), 6.30 (d, *J* = 16.9 Hz, 1H), 5.79 (d, *J* = 9.8 Hz, 1H), 4.77 (s, 2H), 2.62 (s, 2H); ^{13}C NMR (75 MHz, DMSO) δ 167.17, 163.29, 160.19, 158.50, 154.37, 139.57, 137.52, 131.80, 129.27, 127.01, 121.35, 120.90, 117.30, 54.29, 25.56; HRMS *m/z* (ESI): calcd for $C_{19}H_{19}N_7NaO_2$ $[M+Na]^+$ 400.1496, found 400.1498.

*4.1.14. N-(3-(6-((1-(2-hydroxyethyl)-1H-pyrazol-4-yl)amino)pyrimidin-4-yl)phenyl) acrylamide (**6**)*

White solid (yield: 65%). m. p.: 211–213 □. ^{1}H NMR (300 MHz, DMSO) δ 8.83 (s, 1H), 8.13 (s, 1H), 7.89 (s, 1H), 7.71 (d, *J* = 3.3 Hz, 1H), 7.63 (d, *J* = 6.4 Hz, 1H), 7.53 (s, 1H), 7.49 – 7.43 (m, 1H), 7.26 (s, 1H), 6.63 (dd, *J* = 16.9, 10.1 Hz, 1H), 6.29 (d, *J* = 16.8 Hz, 1H), 5.77 (d, *J* = 10.2 Hz, 1H), 4.16 (s, 2H), 3.73 (s, 2 H); ^{13}C NMR (75 MHz, DMSO) δ 163.58, 159.26, 154.57, 154.11, 140.05, 132.98, 131.73, 130.19, 129.68, 127.13, 122.47, 122.07, 120.76, 117.53, 116.91, 102.79, 60.03, 54.40; HRMS *m/z* (ESI): calcd for $C_{18}H_{18}N_6NaO_2$ $[M+Na]^+$ 373.1379, found 373.1377.

*4.1.15. N-(3-(2-((1-(2-methoxyethyl)-1H-pyrazol-4-yl)amino)pyrimidin-4-yl)phenyl) acrylamide (**7**)*

White solid (yield: 69%). m. p.: 189–190 □. ^{1}H NMR (300 MHz, DMSO) δ 8.84 (s, 1H), 8.47 (d, *J* = 4.8 Hz, 1H), 8.21 (s, 1H), 7.79 (d, *J* = 7.4 Hz, 1H), 7.65 (s, 1H), 7.54 (s, 1H), 7.47 (t, *J* = 7.8 Hz, 1H), 7.21 (d, *J* = 4.6 Hz, 1H), 6.54 (dd, *J* = 16.9, 10.0 Hz, 1H), 6.32 (d, *J* = 16.9 Hz, 1H), 5.78 (d, *J* = 10.3 Hz, 1H), 4.33 (s, 2H), 3.70 (t, *J* = 5.2 Hz, 2H), 3.23 (s,3H); ^{13}C NMR (75 MHz, DMSO) δ 163.42, 159.58, 159.02, 139.60, 137.43, 131.87, 129.88, 129.09, 126.79, 123.02, 121.88, 121.44, 120.09, 117.78, 106.44, 70.83, 57.86, 50.98; HRMS *m/z* (ESI): calcd for $C_{19}H_{21}N_6O_2$ $[M+H]^+$ 365.1716, found 365.1711.

*4.1.16. N-(3-(2-((4-morpholinophenyl)amino)pyrimidin-4-yl)phenyl)acrylamide (**8**)*

White solid (yield: 74%). m. p.: 221–224 □. ^{1}H NMR (300 MHz, DMSO) δ 8.55 (s, 1H), 8.50 (d, *J* = 5.1 Hz, 1H), 7.82 (d, *J* = 8.4 Hz, 1H), 7.76 (d, *J* = 6.4 Hz, 2H), 7.69 (d, *J* = 15.7 Hz, 1H), 7.49 (t, *J* = 7.8 Hz, 1H), 7.23 (d, *J* = 5.1 Hz, 1H), 6.98 (d, *J* = 8.3 Hz, 2H), 6.51 (dd, *J* = 16.9, 10.0 Hz, 1H), 6.32 (d, *J* = 16.8 Hz, 1H), 5.80 (d, *J* = 11.4 Hz, 1H), 3.76 (s, 4H), 3.07 (s, 4H); ^{13}C NMR (75 MHz, DMSO) δ 163.47, 163.30, 160.25, 158.90, 139.54, 137.47, 131.83, 129.22, 126.95, 122.00, 121.58, 120.20, 117.87, 115.93, 107.24, 66.05, 49.50; HRMS *m/z* (ESI): calcd for $C_{23}H_{24}N_5O_2$ $[M+H]^+$ 402.1928, found 402.1924.

*4.1.17. N-(4-(6-((1-(2-methoxyethyl)-1H-pyrazol-4-yl)amino)pyrimidin-4-yl)phenyl) acrylamide (**9**)*

White solid (yield: 78%). m. p.: 191–193 □. ^{1}H NMR (300 MHz, DMSO) δ 8.63 (s, 1H), 8.01 (d, *J* = 8.8 Hz, 3H), 7.82 (d, *J* = 8.4 Hz, 2H), 7.55 (s, 1H), 7.04 (s, 1H), 6.48 (dd, *J* = 16.9, 10.0 Hz, 1H), 6.30 (d, *J* = 16.5 Hz, 1H), 5.79 (d, *J* = 10.1 Hz, 1H), 4.25 (t, *J* = 4.9 Hz, 2H), 3.69 (t, *J* = 5.0 Hz, 2H), 3.24 (s, 3H); ^{13}C NMR (75 MHz, DMSO) δ 163.32, 160.14, 158.44, 140.83, 131.89, 131.72, 131.04, 127.20, 127.03, 125.78, 121.92, 120.19, 119.26, 117.41, 99.78, 70.66, 57.94, 51.31; HRMS *m/z* (ESI): calcd for $C_{19}H_{21}N_6O_2$ $[M+H]^+$ 365.1725, found 365.1721.

*4.1.18. N-(4-(6-((4-morpholinophenyl)amino)pyrimidin-4-yl)phenyl)acrylamide (**10**)*

White solid (yield: 80%). m. p.: 248–250 □. ^{1}H NMR (300 MHz, DMSO) δ 8.60 (s, 1H), 7.98 (d, *J* = 7.9 Hz, 2H), 7.82 (d, *J* = 8.1 Hz, 2H), 7.51 (d, *J* = 8.0 Hz, 2H), 7.09 (s, 1H), 6.94 (d, *J* = 8.2 Hz, 2H), 6.48 (dd, *J* = 16.6, 10.1 Hz, 1H), 6.29 (d, *J* = 16.8 Hz, 1H), 5.79 (d, *J* = 9.8 Hz, 1H), 3.74 (s, 4H), 3.06 (s, 4H); ^{13}C NMR (75 MHz, DMSO) δ 163.32, 161.10, 160.22, 158.16, 147.03, 140.87, 131.81, 131.71, 128.61, 127.21, 127.01, 121.67, 119.28, 115.65, 100.19, 66.11, 48.97; HRMS *m/z* (ESI): calcd for $C_{23}H_{24}N_5O_2$ $[M+H]^+$ 402.1923, found 402.1926.

*4.1.19. N-(4-(2-((1-(2-methoxyethyl)-1H-pyrazol-4-yl)amino)pyrimidin-4-yl)phenyl) acrylamide (**11**)*

White solid (yield: 76%). m. p.: 201–203 □. ^{1}H NMR (300 MHz, DMSO) δ 8.43 (d, *J* = 5.1 Hz, 1H), 8.15 (d, *J* = 8.6 Hz, 2H), 8.02 (s, 1H), 7.88 (d, *J* = 8.0 Hz, 2H), 7.60 (s, 1H), 7.23 (d, *J* = 5.2 Hz, 1H), 6.52 (dd, *J* = 16.9, 10.0 Hz, 1H), 6.32 (d, *J* = 16.9 Hz, 1H), 5.79 (d, *J* = 10.2 Hz, 1H), 4.26 (t, *J* = 5.0 Hz, 2H), 3.69 (t, *J* = 5.1 Hz, 2H), 3.27 (s, 3H); ^{13}C NMR (75 MHz, DMSO) δ 163.88, 163.62, 160.16, 159.25, 141.86, 132.17, 130.53, 127.99, 127.74, 123.61, 120.59, 119.71, 106.52, 71.29, 58.41, 51.74; HRMS *m/z* (ESI): calcd for $C_{19}H_{21}N_6O_2$ $[M+H]^+$ 365.1712, found 365.1717.

*4.1.20. N-(4-(2-((4-morpholinophenyl)amino)pyrimidin-4-yl)phenyl)acrylamide (**12**)*

White solid (yield: 82%). m. p.: 210–212 □. ^{1}H NMR (300 MHz, DMSO) δ 8.45 (d, *J* = 5.2 Hz, 1H), 8.15 (d, *J* = 8.6 Hz, 2H), 7.86 (d, *J* = 8.6 Hz, 2H), 7.69 (d, *J* = 8.9 Hz, 2H), 7.28 (d, J = 5.2 Hz, 1H), 6.93 (d, *J* = 8.9 Hz, 2H), 6.51 (dd, *J* = 16.9, 10.0 Hz, 1H), 6.32 (d, *J* = 16.8 Hz, 1H), 5.80 (d, *J* = 11.6 Hz, 1H), 3.79 – 3.70 (m, 4H), 3.08 – 3.02 (m, 4H); ^{13}C NMR (75 MHz, DMSO) δ 163.43, 162.95, 160.32, 158.69, 146.10, 141.43, 133.10, 131.75, 127.56, 127.31, 120.23, 119.25, 115.67, 106.65, 66.20, 49.34; HRMS *m/z* (ESI): calcd for $C_{23}H_{24}N_5O_2$ $[M+H]^+$ 402.1928, found 402.1924.

*4.1.21. N-(3-(6-((1-methyl-1H-pyrazol-4-yl)amino)pyrimidin-4-yl)phenyl)but-2-enam ide (**13**)*

White solid (yield: 80%). m. p.: 193–196 □. ^{1}H NMR (300 MHz, DMSO) δ 8.84 (s, 1H), 8.35 (s, 1H), 8.10 (s, 1H), 7.86 (d, *J* = 5.1 Hz, 1H), 7.71 (s, 1H), 7.58 (d, *J* = 1.6 Hz, 1H), 7.55 – 7.51 (m, 1H), 7.25 (s, 1H), 6.92 – 6.73 (m, 1H), 6.28 (d, *J* = 15.1 Hz, 1H), 3.85 (s, 3H), 1.85 (d, *J* = 4.9 Hz, 3H); ^{13}C NMR (75 MHz, DMSO) δ 163.89, 159.14, 153.31, 151.38, 140.40, 140.28, 131.19, 130.64, 129.68, 125.80, 122.90, 122.62, 121.83, 120.19, 117.35, 103.01, 54.89, 17.50; HRMS *m/z* (ESI): calcd for $C_{18}H_{19}N_6O$ $[M+H]^+$ 335.1615, found 335.1618.

*4.1.22. N-(3-(6-((1-(2-methoxyethyl)-1H-pyrazol-4-yl)amino)pyrimidin-4-yl)phenyl) but-2-enamide (**15**)*

White solid (yield: 82%). m. p.: 188–190 □. ^{1}H NMR (300 MHz, DMSO) δ 8.87 (s, 1H), 8.37 (s, 1H), 8.13 (s, 1H), 7.85 (d, *J* = 5.1 Hz, 1H), 7.76 (s, 1H), 7.60 (d, *J* = 1.6 Hz, 1H), 7.54(t, *J* = 7.6 Hz,1H), 7.25 (s, 1H), 6.92 – 6.73 (m, 1H), 6.28 (d, *J* = 15.1 Hz, 1H), 4.28 (t, *J* = 4.9 Hz, 2H), 3.68 (t, J = 5.0 Hz, 2H), 3.23 (s, 3H). 1.86 (d, *J* = 5.0 Hz, 3H); ^{13}C NMR (75 MHz, DMSO) δ 163.89, 159.24, 153.47, 140.41, 140.33, 131.45, 130.78, 129.73, 125.81, 122.62, 121.85, 120.08, 117.37, 103.04, 70.47, 57.96, 51.50, 17.52; HRMS *m/z* (ESI): calcd for $C_{20}H_{23}N_6O_2$ $[M+H]^+$ 379.1886, found 379.1881.

*4.1.23. N-(3-(6-((4-morpholinophenyl)amino)pyrimidin-4-yl)but-2-enamide (**17**)*

White solid (yield: 85%). m. p.: 257–259 □. ^{1}H NMR (300 MHz, DMSO) δ 8.63 (s, 1H), 8.43 (s, 1H), 7.76 (d, *J* = 7.6 Hz, 1H), 7.68 (d, *J* = 7.3 Hz, 1H), 7.53 (d, *J* = 7.9 Hz, 2H), 7.44 (t, *J* = 7.7 Hz, 1H), 7.12 (s, 1H), 6.95 (d, *J* = 8.1 Hz, 2H), 6.84 (dt, *J* = 21.0, 7.2 Hz, 1H), 6.16 (d, *J* = 15.2 Hz, 1H), 3.74 (s, 4H), 3.06 (s, 4H), 1.88 (d, *J* = 6.7 Hz, 3H); ^{13}C NMR (75 MHz, DMSO) δ 164.10, 161.65, 161.17, 158.77, 147.53, 140.49, 140.33, 138.07, 132.20, 129.68, 126.45, 122.10, 121.53, 121.32, 117.68, 116.14, 101.54, 66.60, 49.47, 17.97; HRMS *m/z* (ESI): calcd for $C_{24}H_{26}N_5O_2$ $[M+H]^+$ 416.2084, found 416.2088.

*4.1.24. N-(3-(6-((1-(2-(dimethylamino)ethyl)-1H-pyrazol-4-yl)amino)pyrimidin-4-yl) phenyl)but-2-enamide (**19**)*

White solid (yield: 66%). m. p.: 197–199 □. ^{1}H NMR (300 MHz, $CDCl_3$) δ 8.60 (s, 2H), 8.05 (s, 1H), 7.84 (s,2H), 7.65 (d, *J* = 6.9 Hz, 1H), 7.53 (d, *J* = 9.5 Hz, 2H), 7.22 (d, *J* = 7.7 Hz, 1H), 6.95 (td, *J* = 13.7, 6.6 Hz, 1H), 6.71 (s, 1H), 5.99 (d, *J* = 15.1 Hz, 1H), 4.18 (t, *J* = 6.3 Hz, 2H), 2.75 (t, *J* = 6.3 Hz, 2H), 2.24 (s, 6H), 1.80 (d, *J* = 6.4 Hz, 3H); ^{13}C NMR (75 MHz, $CDCl_3$) δ 164.85, 162.11, 161.37, 158.40, 141.64, 138.77, 137.98, 133.00, 129.26, 125.41, 123.32, 122.55, 122.02, 118.52, 100.85, 58.90, 50.47, 45.40, 17.79; HRMS *m/z* (ESI): calcd for $C_{21}H_{26}N_7O$ $[M+H]^+$ 392.2194, found 392.2196.

*4.1.25. N-(3-(6-((1-(2-(methylamino)-2-oxoethyl)-1H-pyrazol-4-yl)amino)pyrimidin -4-yl)phenyl)but-2-enami-de (**20**)*

White solid (yield: 66%). m. p.: 224–227 □. ^{1}H NMR (300 MHz, DMSO) δ 8.89 (s, 1H), 8.32 (d, *J* = 29.2 Hz, 2H), 8.18 (s, 1H), 7.86 (d, *J* = 5.4 Hz, 1H), 7.77 (s, 1H), 7.56 (d, *J* = 12.0 Hz, 2H), 7.28 (s, 1H), 6.83 (dt, *J* = 13.5, 5.3 Hz, 1H), 6.28 (d, *J* = 14.9 Hz, 1H), 4.84 (s, 2H), 2.62 (s, 3H), 1.86 (d, *J* = 4.5 Hz, 3H); ^{13}C NMR (75 MHz, DMSO) δ 166.87, 163.89, 159.09, 153.24, 151.11, 140.41, 131.76, 130.43, 129.77, 125.76, 123.67, 122.67, 121.88, 120.19, 117.33, 103.15, 66.97, 25.53, 17.54; HRMS *m/z* (ESI): calcd for $C_{20}H_{21}N_7NaO_2$ $[M+Na]^+$ 414.1645, found 414.1648.

*4.1.26. N-(3-(6-((1-(2-hydroxyethyl)-1H-pyrazol-4-yl)amino)pyrimidin-4-yl)phenyl) but-2-enamide (**21**)*

White solid (yield: 64%). m. p.: 242–244 □. ^{1}H NMR (300 MHz, DMSO) δ 8.87 (s, 1H), 8.36 (s, 1H), 8.15 (s, 1H), 7.87 (d, *J* = 5.8 Hz, 1H), 7.75 (s, 1H), 7.60 (d, *J* = 6.9 Hz, 1H), 7.57 – 7.49 (m, 1H), 7.28 (s, 1H), 6.83 (dt, *J* = 22.5, 7.1 Hz, 1H), 6.29 (d, *J* = 15.0 Hz, 1H), 4.17 (s, 2H), 3.74 (s, 2H), 1.86 (d, *J* = 6.5 Hz, 3H); ^{13}C NMR (75 MHz, DMSO) δ 163.90, 159.14, 153.45, 151.52, 140.37, 131.26, 130.80, 129.74, 125.77, 122.61, 121.82, 119.94, 117.36, 103.06, 59.99, 55.97, 18.49; HRMS *m/z* (ESI): calcd for $C_{19}H_{21}N_6O_2$ $[M+H]^+$ 365.1715, found 365.1719.

*4.1.27. N-(2-((3-(6-((1-(2-methoxyethyl)-1H-pyrazol-4-yl)amino)pyrimidin-4-yl) phenyl)amino)-2-oxoethyl)acrylamide (**24**)*

White solid (yield: 62%). m. p.: 198–199 □. ^{1}H NMR (300 MHz, DMSO) δ 8.83 (s, 1H), 8.57 (s, 1H), 8.28 (s, 1H), 8.11 (s, 1H), 7.74 (d, *J* = 15.0 Hz, 2H), 7.63-7.53 (m, 2H), 7.49 (s, 1H), 6.33 (dd, *J* = 15.2, 8.2 Hz, 1H), 6.12 (d, *J* = 16.8 Hz, 1H), 5.63 (d, *J* = 8.9 Hz, 1H), 4.28 (s, 2H), 4.04 (s, 2H)., 3.68 (s, 2H), 3.23 (s, 3H); ^{13}C NMR (75 MHz, DMSO) δ 168.16, 165.06, 159.46, 154.41, 139.83, 132.17, 131.37, 129.81, 125.62, 122.47, 122.17, 121.85, 117.30, 102.82, 70.49, 57.96, 51.46, 42.74; HRMS *m/z* (ESI): calcd for $C_{21}H_{24}N_7O_3$ $[M+H]^+$ 422.1946, found 422.1941.

*4.1.28. N-(2-((3-(6-((1-(2-methoxyethyl)-1H-pyrazol-4-yl)amino)pyrimidin-4-yl) phenyl)amino)-2-oxoethyl) but-2-enamide (**25**)*

White solid (yield: 66%). m. p.: 185–188 □. ^{1}H NMR (300 MHz, DMSO) δ 8.86 (s, 1H), 8.39 (s, 1H), 8.24 (d, *J* = 15.0 Hz, 1H), 8.12 (s, 1H), 7.77 (s, 1H), 7.74 (s, 1H), 7.59 (s, 1H),7.56 (s, 1H), 7.23 (s, 1H), 6.65 (s, 1H), 6.04 (d, *J* = 14.1 Hz, 1H), 4.28 (s, 2H), 3.94 (d, *J* = 36.3 Hz, 2H)., 3.68 (s, 2H), 3.23 (s, 3H), 1.77 (d, *J* = 17.6 Hz, 3H); ^{13}C NMR (75 MHz, DMSO) δ 168.41, 165.35, 165.22, 159.36, 153.91, 139.91, 139.24, 138.24, 131.44, 129.94, 129.80, 125.51, 122.52, 122.34, 121.88, 117.31,

102.98, 70.48, 57.96, 51.48, 42.74, 17.35; HRMS *m/z* (ESI): calcd for $C_{22}H_{26}N_7O_3$ $[M+H]^+$ 436.2098, found 436.2090.

*4.1.29. N-(2-((3-(6-((4-morpholinophenyl)amino)pyrimidin-4-yl)phenyl)amino)-2-oxoethyl)acrylamide (**26**)*

White solid (yield: 63%). m. p.: 243–245 □. ^{1}H NMR (300 MHz, DMSO) δ 8.64 (s, 1H), 8.52 (s, 1H), 8.37 (s, 1H), 7.69 (d, *J* = 3.9 Hz, 2H), 7.53 (d, *J* = 6.1 Hz, 2H), 7.51 – 7.39 (m, 1H), 7.12 (s, 1H), 6.96 (d, *J* = 6.1 Hz, 2H), 6.37 (dd, *J* = 15.6, 8.4 Hz, 1H), 6.13 (d, *J* = 16.8 Hz, 1H), 5.65 (d, *J* = 8.9 Hz, 1H), 4.01 (s, 2H), 3.74 (s, 4H), 3.06 (s, 4H); ^{13}C NMR (75 MHz, DMSO) δ 167.85, 165.04, 161.07, 158.18, 146.99, 139.42, 137.39, 131.63, 131.38, 129.31, 125.58, 121.52, 121.12, 120.73, 117.04, 115.63, 101.11, 66.08, 55.98, 42.72; HRMS *m/z* (ESI): calcd for $C_{25}H_{27}N_6O_3$ $[M+H]^+$ 459.2144, found 459.2146.

*4.1.30. N-(2-((3-(6-((4-morpholinophenyl)amino)pyrimidin-4-yl)phenyl)amino)-2-oxoethyl)but-2-enamide (**27**)*

White solid (yield: 65%). m. p.: 236–237 □. ^{1}H NMR (300 MHz, DMSO) δ 8.63 (s, 1H), 8.36 (s, 1H), 8.20 (s, 1H), 7.69 (d, *J* = 1.2 Hz, 2H), 7.52 (d, *J* = 8.3 Hz, 2H), 7.45 (t, *J* = 7.8 Hz, 1H), 7.12 (s, 1H), 6.94 (d, *J* = 8.3 Hz, 2H), 6.76 – 6.60 (m, 1H), 6.05 (d, *J* = 15.3 Hz, 1H), 3.99 (d, *J* = 5.6 Hz, 2H), 3.74 (s, 4H), 3.06 (s, 4H), 1.82 (d, *J* = 6.6 Hz, 3H); ^{13}C NMR (75 MHz, DMSO) δ 168.04, 165.40, 161.18, 160.67, 158.29, 147.06, 139.41, 138.22, 137.62, 131.69, 129.21, 125.57, 121.66, 121.14, 120.79, 117.21, 115.65, 101.04, 66.11, 48.99, 42.77, 17.30; HRMS *m/z* (ESI): calcd for $C_{26}H_{28}N_6NaO_3$ $[M+Na]^+$ 495.2117, found 495.2118.

*4.1.31. N-(3-(2-((4-morpholinophenyl)amino)pyrimidin-4-yl)but-2-enamide (**30**)*

White solid (yield: 83%). m. p.: 264–265 □. ^{1}H NMR (300 MHz, DMSO) δ 8.63 (s, 1H), 8.49 (s, 1H), 7.87 (d, *J* = 5.2 Hz, 1H), 7.77 (s, 3H), 7.44 (s, 1H), 7.22 (s, 1H), 7.16 (s, 1H), 6.97 – 6.72 (m, 2H), 6.38 (d, *J* = 14.6 Hz, 1H), 3.81 (s, 4H), 3.15 (s, 4H), 1.84 (s, 3H); ^{13}C NMR (75 MHz, DMSO) δ 163.80, 163.72, 160.03, 158.77, 144.04,

140.10, 139.57, 137.14, 129.04, 126.23, 123.35, 121.56, 120.05, 117.80, 117.20, 107.52, 65.49, 50.49, 17.50; HRMS *m/z* (ESI): calcd for $C_{24}H_{26}N_5O_2$ $[M+H]^+$ 416.2084, found 416.2080.

*4.1.32. N-(4-(6-((1-(2-methoxyethyl)-1H-pyrazol-4-yl)amino)pyrimidin-4-yl)phenyl) but-2-enamide (**32**)*

White solid (yield: 84%). m. p.: 219–220 □. ^{1}H NMR (300 MHz, DMSO) δ 8.63 (s, 1H), 8.02 (d, *J* = 5.5 Hz, 2H), 7.98 (s, 1H), 7.80 (d, *J* = 8.6 Hz, 2H), 7.56 (s, 1H), 7.04 (s, 1H), 6.84 (dq, *J* = 13.8, 6.7 Hz, 1H), 6.17 (d, *J* = 15.2 Hz, 1H), 4.25 (t, *J* = 5.2 Hz, 2H), 3.68 (t, *J* = 5.2 Hz, 2H), 3.24 (s, 3H), 1.87 (d, *J* = 6.6 Hz, 3H); ^{13}C NMR (75 MHz, DMSO) δ 163.61, 160.17, 158.40, 141.13, 140.24, 131.54, 130.94, 126.94, 125.86, 121.89, 121.55, 119.10, 99.68, 70.63, 57.90, 51.29, 17.44; HRMS *m/z* (ESI): calcd for $C_{20}H_{23}N_6O_2$ $[M+H]^+$ 379.1877, found 379.1878.

*4.1.33. N-(4-(6-((4-morpholinophenyl)amino)pyrimidin-4-yl)but-2-enamide (**34**)*

White solid (yield: 86%). m. p.: 276–277 □. ^{1}H NMR (300 MHz, DMSO) δ 8.59 (s, 1H), 7.97 (d, *J* = 8.5 Hz, 2H), 7.80 (d, *J* = 8.6 Hz, 2H), 7.51 (d, *J* = 8.7 Hz, 2H), 7.08 (s, 1H), 6.93 (d, *J* = 8.8 Hz, 2H), 6.83 (dt, *J* = 14.0, 7.0 Hz, 1H), 6.16 (d, *J* = 15.0 Hz, 1H), 3.76 – 3.71 (m, 4H), 3.08 – 3.02 (m, 4H), 1.88 (d, *J* = 6.6 Hz, 3H); ^{13}C NMR (75 MHz, DMSO) δ 163.62, 161.08, 160.42, 158.22, 146.97, 141.14, 140.27, 131.75, 131.60, 126.92, 125.86, 121.63, 119.12, 115.63, 100.08, 66.09, 48.97, 17.46; HRMS *m/z* (ESI): calcd for $C_{24}H_{26}N_5O_2$ $[M+H]^+$ 416.2080, found 416.2087.

*4.1.34. N-(4-(2-((1-(2-methoxyethyl)-1H-pyrazol-4-yl)amino)pyrimidin-4-yl)phenyl) but-2-enamide (**36**)*

White solid (yield: 85%). m. p.: 212–215 □. ^{1}H NMR (300 MHz, DMSO) δ 8.93 (d, *J* = 5.7 Hz, 1H), 8.18 (d, *J* = 8.4 Hz, 2H), 8.07 (s, 1H), 7.96 (d, *J* = 7.9 Hz, 2H), 7.68 (s, 1H), 7.55 (d, *J* = 5.3 Hz, 1H), 6.82 (dt, *J* = 13.5, 6.7 Hz, 1H), 6.33 (d, *J* = 15.2 Hz, 1H), 4.30 (s, 2H), 3.69 (s, 2H), 3.26 (s, 3H), 1.85 (d, *J* = 6.6 Hz, 3H); ^{13}C NMR (75 MHz, DMSO) δ 164.06, 155.35, 153.58, 144.11, 140.69, 140.55, 129.20, 128.66,

127.88, 125.88, 124.03, 119.26, 119.14, 105.95, 70.57, 58.00, 51.46, 17.53; HRMS *m/z* (ESI): calcd for $C_{20}H_{23}N_6O_2$ $[M+H]^+$ 379.1882, found 379.1885.

*4.1.35. N-(4-(2-((4-morpholinophenyl)amino)pyrimidin-4-yl)but-2-enamide (**38**)*

White solid (yield: 86%). m. p.: 268–271 □. ^{1}H NMR (300 MHz, DMSO) δ 8.42 (s, 1H), 8.12 (d, *J* = 7.3 Hz, 2H), 7.83 (d, *J* = 7.4 Hz, 2H), 7.68 (d, *J* = 7.5 Hz, 2H), 7.25 (s, 1H), 6.92 (d, *J* = 7.5 Hz, 2H), 6.83 (d, *J* = 7.0 Hz, 1H), 6.17 (d, *J* = 15.0 Hz, 1H), 3.73 (s, 4H), 3.03 (s, 4H), 1.88 (d, *J* = 4.7 Hz, 3H); ^{13}C NMR (75 MHz, DMSO) δ 164.17, 163.44, 160.75, 159.06, 146.54, 142.16, 140.87, 133.55, 131.78, 127.93, 126.33, 120.67, 119.55, 116.10, 107.03, 66.63, 49.78, 17.95; HRMS *m/z* (ESI): calcd for $C_{24}H_{26}N_6O_3$ $[M+H]^+$ 416.2080, found 416.2084.

Method B: General procedure for the synthesis of targets **14**, **16**, **18**, **22-23**, **28-29**, **31**, **33**, **35**, **37**, and **39**.

To a stirred solution of **42a** (0.1 g, 0.37 mmol) in THF (15 mL) were added DIEA (0.12 g, 0.94 mmol), o-(7-azabenzotriazol-1-yl)-*N*,*N*,*N'*,*N'*-tetramethyluronium hexafluorophosphate (HATU, 0.35 g, 0.94 mmol), and 2-cyanoacetic acid (0.03 g, 0.41 mmol) at 0□. The reaction mixture was stirred at room temperature for 16 h. It was quenched with water and extracted with ethyl acetate. The organic layer was washed with water followed by brine, dried over anhydrous sodium sulfate, and was evaporated to dryness. The crude mass was purified by silica gel column chromatography (DCM: MeOH = 20:1) to afford the title compounds.

*4.1.36. 2-cyano-N-(3-(6-((1-methyl-1H-pyrazol-4-yl)amino)pyrimidin-4-yl)phenyl)acetamide (**14**)*

White solid (yield: 95%). m. p.: 193–195 □. ^{1}H NMR (300 MHz, DMSO) δ 8.66 (s, 1H), 8.33 (s, 1H), 8.02 (s, 1H), 7.73 (d, *J* = 7.5 Hz, 1H), 7.64 (d, *J* = 7.1 Hz, 1H), 7.53 (s, 1H), 7.47 (t, *J* = 7.9 Hz, 1H), 7.07 (s, 1H), 3.94 (s, 2H), 3.83 (s, 2H); ^{13}C NMR (75 MHz, DMSO) δ 161.27, 158.28, 138.89, 137.40, 129.47, 121.78, 120.84, 117.15,

115.84, 56.00, 26.79; HRMS *m/z* (ESI): calcd for $C_{17}H_{16}N_7O$ $[M+H]^+$ 334.1419, found 334.1414.

*4.1.37. 2-Cyano-N-(3-(6-((1-(2-methoxyethyl)-1H-pyrazol-4-yl)amino)pyrimidin-4-yl) phenyl)acetamide (**16**)*

White solid (yield: 94%). m. p.: 186–188 □. ^{1}H NMR (300 MHz, DMSO) δ 8.66 (s, 1H), 8.34 (s, 1H), 8.03 (s, 1H), 7.74 (d, *J* = 7.6 Hz, 1H), 7.65 (d, *J* = 7.7 Hz, 1H), 7.56 (s, 1H), 7.47 (t, *J* = 7.9 Hz, 1H), 7.07 (s, 1H), 4.25 (t, *J* = 5.0 Hz, 2H), 3.94 (s, 2H), 3.68 (t, *J* = 5.0 Hz, 2H), 3.23 (s, 3H); ^{13}C NMR (75 MHz, DMSO) δ 161.71, 160.71, 159.01, 139.36, 138.16, 131.34, 129.89, 122.26, 121.31, 117.73, 116.27, 101.44, 71.13, 58.40, 51.82, 27.23; HRMS *m/z* (ESI): calcd for $C_{19}H_{20}N_7O_2$ $[M+H]^+$ 378.1676, found 378.1673.

*4.1.38. 2-Cyano-N-(3-(6-((4-morpholinophenyl)amino)pyrimidin-4-yl)phenyl)acetami de (**18**)*

White solid (yield: 94%). m. p.: 211–213 □. ^{1}H NMR (300 MHz, DMSO) δ 8.63 (s, 1H), 8.33 (s, 1H), 7.72 (d, *J* = 6.9 Hz, 1H), 7.64 (d, *J* = 8.1 Hz, 1H), 7.52 (d, *J* = 8.2 Hz, 2H), 7.49 – 7.44 (m, 1H), 7.12 (s, 1H), 6.95 (d, *J* = 8.1 Hz, 2H), 3.94 (s, 2H), 3.74 (s, 4H), 3.07 (s, 4H); ^{13}C NMR (75 MHz, DMSO) δ 161.73, 161.64, 160.86, 158.84, 147.55, 139.40, 138.21, 132.14, 129.95, 122.22, 122.12, 121.31, 117.66, 116.31, 116.14, 101.65, 66.60, 49.45, 27.29; HRMS *m/z* (ESI): calcd for $C_{23}H_{23}N_6O_2$ $[M+H]^+$ 415.1888, found 459.1883.

*4.1.39. 2-Cyano-N-(3-(6-((1-(2-hydroxyethyl)-1H-pyrazol-4-yl)amino)pyrimidin-4-yl) phenyl)acetamide (**22**)*

White solid (yield: 95%). m. p.: 194–195 □. ^{1}H NMR (300 MHz, DMSO) δ 8.66 (s, 1H), 8.34 (s, 1H), 8.05 (s, 1H), 7.74 (d, *J* = 7.5 Hz, 1H), 7.65 (d, *J* = 7.7 Hz, 1H), 7.55 (s, 1H), 7.48 (t, *J* = 7.9 Hz, 1H), 7.08 (s, 1H), 4.14 (t, *J* = 5.4 Hz, 2H), 3.95 (s, 2H), 3.81 – 3.71 (m, 2H); ^{13}C NMR (75 MHz, DMSO) δ 161.23, 159.94, 158.54, 138.89,

137.65, 130.40, 129.43, 121.73, 120.77, 117.17, 115.81, 101.05, 60.19, 54.26, 26.79; HRMS *m/z* (ESI): calcd for $C_{18}H_{17}N_7NaO_2$ $[M+Na]^+$ 386.1348, found 386.1344.

*4.1.40. 2-Cyano-N-(2-((3-(6-((1-methyl-1H-pyrazol-4-yl)amino)pyrimidin-4-yl)phenyl) amino)-2-oxoethyl)acetamide (**23**)*

White solid (yield: 83%). m. p.: 213–214 □. ^{1}H NMR (300 MHz, DMSO) δ 8.65 (d, *J* = 6.0 Hz, 2H), 8.34 (s, 1H), 8.01 (s, 1H), 7.70 (d, *J* = 6.0 Hz, 2H), 7.53 (s, 1H), 7.46 (t, *J* = 6.0 Hz, 1H), 7.07 (s, 1H), 3.98 (d, *J* = 5.6 Hz, 2H), 3.84 (s, 3H), 3.77 (s, 2H); ^{13}C NMR (75 MHz, DMSO) δ 167.26, 162.79, 160.05, 158.33, 139.22, 137.34, 129.30, 121.35, 120.92, 117.29, 116.08, 101.13, 43.08, 38.72, 25.21; HRMS *m/z* (ESI): calcd for $C_{19}H_{19}N_8O_2$ $[M+H]^+$ 391.1636, found 391.1630.

*4.1.41. 2-Cyano-N-(2-((3-(6-((4-morpholinophenyl)amino)pyrimidin-4-yl)phenyl) amino)-2-oxoethyl)acetamide (**28**)*

White solid (yield: 88%). m. p.: 257–259 □. ^{1}H NMR (300 MHz, DMSO) δ 8.63 (s, 2H), 8.33 (s, 1H), 7.67 (s, 2H), 7.50 (d, *J* = 8.5 Hz, 2H), 7.48 – 7.41 (m, 1H), 7.10 (s, 1H), 6.92 (d, *J* = 8.6 Hz, 2H), 3.97 (d, *J* = 5.2 Hz, 2H), 3.75 (s, 2H), 3.72 (s, 4H), 3.04 (s, 4H); ^{13}C NMR (75 MHz, DMSO) δ 167.28, 162.81, 161.07, 160.08, 158.06, 147.05, 139.25, 137.24, 131.51, 129.35, 121.61, 121.31, 120.94, 117.20, 116.11, 115.61, 101.13, 66.07, 48.88, 43.05, 25.20; HRMS *m/z* (ESI): calcd for $C_{25}H_{25}N_7NaO_3$ $[M+Na]^+$ 494.1912, found 494.1917.

*4.1.42. 2-Cyano-N-(2-((3-(6-((1-(2-(methylamino)-2-oxoethyl)-1H-pyrazol-4-yl) amino)pyrimidin-4-yl)phenyl)amino)-2-oxoethyl)acetamide (**29**)*

White solid (yield: 82%). m. p.: 223–224 □. ^{1}H NMR (300 MHz, DMSO) δ 8.66 (s, 2H), 8.36 (s, 1H), 8.07 (s, 1H), 7.98 (d, *J* = 3.0 Hz, 1H), 7.57 (s, 1H), 7.50 (d, *J* = 4.1 Hz, 1H), 7.49 – 7.45 (m, 1H), 7.10 (s, 1H), 4.76 (s, 2H), 3.97 (d, *J* = 5.5 Hz, 2H), 3.77 (s, 2H), 2.62 (d, *J* = 4.4 Hz, 3H); ^{13}C NMR (75 MHz, DMSO) δ 167.24, 167.16, 162.75, 160.30, 158.48, 150.83, 139.25, 137.56, 131.30, 122.21, 121.31, 120.92,

120.53, 117.37, 116.04, 101.00, 54.34, 43.10, 25.55, 25.19; HRMS *m/z* (ESI): calcd for $C_{21}H_{22}N_9O_3$ $[M+H]^+$ 448.1844, found 448.1842.

*4.1.43. 2-Cyano-N-(3-(2-((4-morpholinophenyl)amino)pyrimidin-4-yl)phenyl) acetamide (**31**)*

White solid (yield: 94%). m. p.: 217–218 □. ^{1}H NMR (300 MHz, DMSO) δ 8.61 (s, 1H), 8.50 (d, *J* = 5.0 Hz, 1H), 7.83 (d, *J* = 7.7 Hz, 1H), 7.77 (d, *J* = 8.5 Hz, 2H), 7.68 (d, *J* = 8.0 Hz, 1H), 7.48 (t, *J* = 7.8 Hz, 1H), 7.25 (d, *J* = 4.9 Hz, 1H), 7.06 (d, *J* = 5.9 Hz, 2H), 4.08 (s, 2H), 3.77 (s, 4H), 3.10 (s, 4H); ^{13}C NMR (75 MHz, DMSO) δ 163.25, 161.28, 160.16, 158.96, 139.09, 137.43, 129.25, 122.29, 121.49, 120.47, 120.15, 117.74, 116.29, 115.92, 107.22, 65.87, 49.74, 26.66; HRMS *m/z* (ESI): calcd for $C_{23}H_{23}N_6O_2$ $[M+H]^+$ 415.1880, found 415.1882.

*4.1.44. 2-Cyano-N-(4-(6-((1-(2-methoxyethyl)-1H-pyrazol-4-yl)amino)pyrimidin-4-yl) phenyl)acetamide (**33**)*

White solid (yield: 96%). m. p.: 192–194 □. ^{1}H NMR (300 MHz, DMSO) δ 8.63 (s, 1H), 8.01 (d, *J* = 8.0 Hz, 3H), 7.69 (d, *J* = 8.5 Hz, 2H), 7.55 (s, 1H), 7.02 (s, 1H), 4.25 (t, *J* = 5.2 Hz, 2H), 3.94 (s, 2H), 3.68 (t, *J* = 5.2 Hz, 2H), 3.24 (s, 3H); ^{13}C NMR (75 MHz, DMSO) δ 161.22, 160.36, 159.98, 158.40, 140.09, 132.27, 130.91, 127.12, 121.82, 121.58, 119.15, 115.71, 99.94, 70.62, 57.90, 51.29, 26.80; HRMS *m/z* (ESI): calcd for $C_{19}H_{20}N_7O_2$ $[M+H]^+$ 378.1673, found 378.1676.

*4.1.45. 2-Cyano-N-(4-(6-((4-morpholinophenyl)amino)pyrimidin-4-yl)phenyl) acetamide (**35**)*

White solid (yield: 95%). m. p.: 240–241 □. ^{1}H NMR (300 MHz, DMSO) δ 8.60 (s, 1H), 8.00 (d, *J* = 8.3 Hz, 2H), 7.70 (d, *J* = 8.2 Hz, 2H), 7.50 (d, *J* = 8.4 Hz, 2H), 7.08 (s, 1H), 6.92 (d, *J* = 8.4 Hz, 2H), 3.94 (s, 2H), 3.72 (s, 4H), 3.04 (s, 4H); ^{13}C NMR (75 MHz, DMSO) δ 161.26, 161.15, 160.24, 158.25, 147.08, 140.15, 132.36, 131.66, 127.14, 121.77, 119.24, 115.66, 100.29, 66.12, 48.98, 26.83; HRMS *m/z* (ESI): calcd for $C_{23}H_{23}N_6O_2$ $[M+H]^+$ 415.1888, found 415.1885.

*4.1.46. 2-Cyano-N-(4-(2-((1-(2-methoxyethyl)-1H-pyrazol-4-yl)amino)pyrimidin-4-yl) phenyl)acetamide (**37**)*

White solid (yield: 96%).m. p.: 225–228 □. ^{1}H NMR (300 MHz, DMSO) δ 8.44 (d, *J* = 5.1 Hz, 1H), 8.15 (d, *J* = 8.5 Hz, 2H), 8.01 (s, 1H), 7.74 (d, *J* = 8.5 Hz, 2H), 7.60 (s, 1H), 7.22 (d, *J* = 5.2 Hz, 1H), 4.25 (t, *J* = 4.8 Hz, 2H), 3.96 (s, 2H), 3.69 (t, *J* = 5.0 Hz, 2H), 3.26 (s, 3H); ^{13}C NMR (75 MHz, DMSO) δ 163.06, 161.38, 159.76, 158.91, 140.67, 132.19, 130.14, 127.67, 123.15, 120.16, 119.18, 115.77, 106.15, 70.86, 57.98, 51.31, 26.91; HRMS *m/z* (ESI): calcd for $C_{19}H_{20}N_7O_2$ $[M+H]^+$ 378.1677, found 378.1679.

*4.1.47. 2-Cyano-N-(4-(2-((4-morpholinophenyl)amino)pyrimidin-2-yl)phenyl) acetamide (**39**)*

White solid (yield: 95%). m. p.: 267–269 □. ^{1}H NMR (300 MHz, DMSO) δ 8.44 (d, *J* = 5.0 Hz, 1H), 8.14 (d, *J* = 8.4 Hz, 2H), 7.73 (d, *J* = 8.5 Hz, 2H), 7.68 (d, *J* = 8.8 Hz, 2H), 7.26 (d, *J* = 5.0 Hz, 1H), 6.92 (d, *J* = 8.6 Hz, 2H), 3.96 (s, 2H), 3.73 (s, 4H), 3.03 (s, 4H); ^{13}C NMR (75 MHz, DMSO) δ 163.27, 161.81, 160.73, 159.17, 146.51, 141.12, 133.50, 132.52, 128.10, 120.67, 119.57, 116.20, 116.11, 107.12, 66.61, 49.76, 27.34; HRMS *m/z* (ESI): calcd for $C_{23}H_{23}N_6O_2$ $[M+H]^+$ 415.1887, found 415.1880.

4.2. Bioactivity

4.2.1. Mice

Female BALB/c mice (6-8 weeks) were used for modeling DTH and T cell experiments. Male ICR mice (6-8 weeks, body weight 20-22g) were used in PK studies of compound **12**. Mice were purchased from the laboratory animal center of Beijing Huafukang Biological Technology Co., Ltd, (Beijing, China), and were acclimatized at a controlled temperature of 20-22°C, and a relative humidity of 50-60% under a 12 h light-dark condition. All animal procedures were approved by the Animal Care and Use Committee of Institute of Materia Medica, Chinese Academy of

Medical Sciences and Peking Union Medical College (CAMS & PUMC, Beijing, China).

4.2.2. Biochemical assays-JAK enzymatic inhibition assay (Cell-free kinase activity assays)

Cell-free kinase (JAK1, JAK2 JAK3, and TYK2, purchased from Invitrogen (Thermo Fisher Scientific, Waltham, Massachusetts, USA) assays were performed using the HTRF KinEASE-TK (Cisbio Bioassays, Codolet, France) method as previously described [24]. Compounds were screened at serial dilution in the presence of 2% DMSO with a 5-min pre-incubation of kinase and compounds. All reactions started by the addition of ATP and TK-substrate-biotin, incubations were performed at room temperature for 30 min and quenched with stop solution, containing 25 nM Strep-XL665 and TK Ab-Cryptate. Plates were incubated for 1 h before being read on synergy H1 (Biotek Instruments, Winooski, Vermont, USA) using standard HTRF settings. The half maximal inhibitory concentration (IC_{50}) was calculated by nonlinear regression using GraphPad Prism 8.0 software.

4.2.3. T cell isolation

T cells were purified from single-cell suspensions of spleen and lymph nodes from male and female mice aged 6–8 weeks by negative selection using biotinylated antibodies directed to CD8a, CD11b, CD11c, CD19, CD24, CD45R/B220, CD49b, CD105, I-A/I-E (MHC-II), TER-119/Erythroid, TCR-γδ (all BioLegend, San Diego, CA,USA) and magnetic Streptavidin Nanobeads (BioLegend).

4.2.4. Cell viability assays

Resting naive T cells, IL-4-treated activated T cells, and RAW264.7 cells were used to determine the cell viability of compounds using the MTS Assay (Promega, Madison, WI, USA) according to the manufacturer's guidelines. Briefly, purified T cells were stimulated with Ultra-LEAF™ Purified anti-CD3/ Ultra-LEAF™ Purified anti-CD28 Biolegend for 72 h, washed with RPMI 1640 medium (Gibco, Thermo

Fisher Scientific), and treated with 10 ng/ml of IL-4 (PeproTech, Rocky Hill, NJ, USA) for 48 h. Purified resting T cells (10^6 cells/mL), IL-4-treated activated T cells (10^6 cells/ml), and Raw264.7 cells (5 x 10^5cells/mL) were treated with vehicle (0.1% DMSO) alone or 10 μM of different compounds for 72 h. The viability of cells was evaluated using the MTS kit by measuring the absorbance at 490 nm in a microplate reader synergy H1 (Biotek). Values were presented as the percent cell viability relative to the vehicle control.

4.2.5. T cell proliferation

T cells were adjusted to 10^6 cells per mL in complete RPMI1640 medium. Next, cells were exposed to anti-CD3/anti-CD28 or IL-2 (Peprotech) in 96-well culture microtiter plates in triplicate. Complete RPMI1640 medium lacking an-CD3/anti-CD28 or IL-2 was used as the control. Cells were incubated at 37 °C in a humidified, 5% CO_2 incubator for 72 h. Subsequently, the cell viability was monitored using the MTS assay. Values were transformed to the percent inhibition relative to the vehicle control, and IC_{50} curves were created based on nonlinear regression analysis of the data using GraphPad Prism 8.0 software.

4.2.6. Western blot analysis

For cytokine stimulation, purified T cells were pre-activated in 96-well plates coated with anti-CD3 and anti-CD28 for 72 h, harvested, cultured with IL-2 (50 U/mL, Peprotech) for 36 h, then, cultured without IL-2 for 36 h before all experiments.

Equal numbers of T cells (10^6 cells/mL) were incubated at the indicated concentration of compounds in DMSO or DMSO alone (control) for 1 h, then stimulated with either IL-2 (50 ng/mL; Peprotech) or IL-15 (50 ng/mL; Peprotech) for 30 min. After stimulation, cells were lysed in cell lysis buffer containing Phenyl methane sulfonyl fluoride (PMSF), complete protease inhibitors and phosphatase inhibitors (Cell signaling technology, Danvers, MA, USA). Protein lysates were quantified by BCA assay (Thermo Fisher Scientific). Equal amounts of total protein (20 μg) were separated by SDS PAGE, transferred to PVDF membranes, followed by

membrane blocking with 5% Bovine Serum Albumin buffer (BSA, Sigma-Aldrich, St, Louis, MO, USA) overnight incubation at 4 °C with Abs recognizing STAT5, anti-phospho-Stat5 Tyr694 (Cell Signaling technology) and followed by secondary horseradish peroxidase (HRP)-conjugated antibodies (Cell Signaling technology). Protein bands were visualized by enhanced chemi luminescence (ECL) reagents from Merck Millipore (Belize, USA) and their intensities were quantified using ImageJ Software (NIH, Bethesda, MD, USA).

4.2.7. Kinase selectivity profiling

Selectivity profiling of compound **12** (100 nM) was performed at Thermos Fisher (Invitrogen) by using Select Screen® Kinase Profiling by at the Km concentration of ATP of each kinase.

*4.2.8. Time assay and dissociation kinetics of compound **12***

Compound **12** and tofacitinib or kinase buffer (positive control) were incubated with recombinant JAK3 for various periods of time (0, 2, 5, 10, 15, 20, 30, 40, and 60 min) before ATP, and the substrate was added to initiate the kinase reaction. The stop reactions were kept constant according to HTRF KinEASE-TK assays. Inhibition rate values were plotted versus incubation time using GraphPad Prism 8.0 software.

Dissociation kinetics of compound **12** was measured by incubating 2000 nM JAK3 with inhibitors at their IC_{90} for 30 minutes. Activity was measured as above after a 1000-fold dilution into reaction buffer at an ATP equivalent to its Km. The corresponding HTRF ratios were measured for various periods of time (0, 1, 2, 8, and 24 hours) and were calculated as follows: (Signal 665 nm)/(Signal 620 nm) x10000. The corresponding HTRF ratio values were plotted versus time using GraphPad Prism 8.0 software.

4.2.9. In vivo pharmacokinetic study

For *in vivo* pharmacokinetic studies, male ICR mice (n = 6), were fasted overnight and received a single dose (30 mg/kg) of compound **12** (dissolved in 5% DMSO and

95% sodium carboxyl methyl cellulose) by oral gavage, Intravenous administration was given at 10% DMSO in saline (10 mg/kg). Blood samples (50 μL) were obtained from the orbital venous sinus at 0 min, 5 min, 10 min, 20 min, 30 min, 45 min, 1 h, 2 h, 4 h, 6 h, 8 h, 10 h, 12 h, 24 h, and 48 h after compound administration. The concentration of corresponding compounds in blood was analyzed by LC-MS/MS (8050, Shimadzu, Japan), and pharmacokinetic parameters were processed by DAS 3.0 software using each time point and the concentration of corresponding compounds.

4.2.10. In vivo efficacy studies

Animals (n = 5 per group for treated mice and n = 3 for control) were sensitized on the abdomen and subsequently challenged on the pinna with OXZ (E0753, Sigma-Aldrich, St, Louis, MO, USA). Compounds (30 mg/kg, by p.o.) or the positive control (tofacitinib, 30 mg/kg) were administered just prior to and during the challenge phase. The left ear served as an internal control. After the final boost, mice were sacrificed through cervical dislocation, each ear was collected with a cork borer with a diameter of 8 mm and quickly weighed. Then, sections of the right ear were immediately fixed in 10% paraformaldehyde solution for 72 h and HE-staining was performed. Changes in ear weight were calculated as the right ear weight-left ear weight. Ear swelling (%) was calculated by the following formula: Ear swelling (%) = (ear weight-left ear weight)/left ear weight x100%. Spleens were isolated and the spleen index was calculated as organ weight 10 milligram (mg) per gram (g) of mouse body weight.

4.3. Computational analysis

For computational analysis, we used the X-ray co-crystal structure of JAK3 in the Protein Data Bank (PDB code: 4Z16) [24]. The protein structure for the docking studies was prepared using the Protein Preparation Workflow. All crystallographic waters were removed and chain A was kept. Hybridization states, charges, and angles were assigned in the protein structure with missing bond orders, and hydrogen atoms

were added. Docking grids were generated and defined based on the centroid of compound **12** in the ATP binding site incorporating hydrogen-bond constraints to the hinge and hydrophobic regions. Ligands were prepared using Molecular Operating Environment (MOE) software. Energy-minimized conformation of each ligand was used to docking calculation input molecules. In this study, Ligand-Fit and CDOCKER docking programs implemented in MOE software were used [32]. Other docking parameters were kept at default values. The top-scoring pose was employed for discussions.

4.4. Statistics

Statistical analyses were performed using GraphPad Prism 8.0 software. Results are expressed as the mean ± SEM of at least 3 independent experiments. The differences of multiple comparisons were analyzed using one-way ANOVA, followed by an appropriate post hoc test and p value < 0.05 was considered statistically significant.

Conflicts of interest

The authors declared that they have no conflicts of interest.

Acknowledgments

The authors are grateful to financial supports from National Natural science Foundation of China (30973607, 81172934), "Double First-Class" New Drug Development Project of China Pharmaceutical University (CPU2018PZQ15), the Beijing Municipal Natural Science Foundation (7182115), CAMS Innovation Fund for Medical Science (2017-I2M-3-011) and Drug Innovation Major Project of China, China (No. 2018ZX09711001-003-001)

Appendix A. Supplementary data

Supplementary data to this article can be found online at

References

[1] M. Gadina, C. Johnson, D. Schwartz, M. Bonelli, S. Hasni, Y. Kanno, P. Changelian, A. Laurence, J.J. O'Shea, Translational and clinical advances in JAK-STAT biology: The present and future of jakinibs, J Leukoc Biol, 104 (2018) 499-514.

[2] M. Mavers, E.M. Ruderman, H. Perlman, Intracellular signal pathways: potential for therapies, Curr. Rheumatol. Rep. 11 (2009) 378-385.

[3] O'Shea, J. J.; Gadina, M.; Schreiber, R. D. Cytokine signaling in 2002: new surprises in the Jak/Stat pathway. Cell 2002, 109

[4] K. Ghoreschi, A. Laurence, J.J. O'Shea, Janus kinases in immune cell signaling, Immunol Rev, 228 (2009) 273-287.

[5] K. Kaur, S. Kalra, S. Kaushal, Systematic review of tofacitinib: a new drug for the management of rheumatoid arthritis, Clin. Ther. 36 (2014) 1074-1086.

[6] J.P. Malerich, J.S. Lam, B. Hart, R.M. Fine, B. Klebansky, M.J. Tanga, A. D'Andrea, Diamino-1,2,4-triazole derivatives are selective inhibitors of TYK2 and JAK1 over JAK2 and JAK3, Bioorg. Med. Chem. Lett. 20 (2010) 7454-7457.

[7] J.S. Fridman, P.A. Scherle, R. Collins, T.C. Burn, Y. Li, J. Li, M.B. Covington, B. Thomas, P. Collier, M.F. Favata, X. Wen, J. Shi, R. McGee, P.J. Haley, S. Shepard, J.D. Rodgers, S. Yeleswaram, G. Hollis, R.C. Newton, B. Metcalf, S.M. Friedman, K. Vaddi, Selective inhibition of JAK1 and JAK2 is efficacious in rodent models of arthritis: preclinical characterization of INCB028050, J. Immunol. 184 (2010) 5298-5307.

[8] J.M. Parmentier, J. Voss, C. Graff, A. Schwartz, M. Argiriadi, M. Friedman, H.S. Camp, R.J. Padley, J.S. George, D. Hyland, M. Rosebraugh, N. Wishart, L. Olson, A.J. Long, In vitro and in vivo characterization of the JAK1 selectivity of upadacitinib (ABT-494), BMC Rheumatol, 2 (2018) 23.

[9] H. Hamaguchi, Y. Amano, A. Moritomo, S. Shirakami, Y. Nakajima, K. Nakai, N. Nomura, M. Ito, Y. Higashi, T. Inoue, Discovery and structural characterization of

peficitinib (ASP015K) as a novel and potent JAK inhibitor, Bioorg. Med. Chem. 26 (2018) 4971-4983.

[10] P.S. Changelian, M.E. Flanagan, D.J. Ball, C.R. Kent, K.S. Magnuson, W.H. Martin, B.J. Rizzuti, P.S. Sawyer, B.D. Perry, W.H. Brissette, S.P. McCurdy, E.M. Kudlacz, M.J. Conklyn, E.A. Elliott, E.R. Koslov, M.B. Fisher, T.J. Strelevitz, K. Yoon, D.A. Whipple, J. Sun, M.J. Munchhof, J.L. Doty, J.M. Casavant, T.A. Blumenkopf, M. Hines, M.F. Brown, B.M. Lillie, C. Subramanyam, C. Shang-Poa, A.J. Milici, G.E. Beckius, J.D. Moyer, C. Su, T.G. Woodworth, A.S. Gaweco, C.R. Beals, B.H. Littman, D.A. Fisher, J.F. Smith, P. Zagouras, H.A. Magna, M.J. Saltarelli, K.S. Johnson, L.F. Nelms, S.G. Des Etages, L.S. Hayes, T.T. Kawabata, D. Finco-Kent, D.L. Baker, M. Larson, M.S. Si, R. Paniagua, J. Higgins, B. Holm, B. Reitz, Y.J. Zhou, R.E. Morris, J.J. O'Shea, D.C. Borie, Prevention of organ allograft rejection by a specific Janus kinase 3 inhibitor, Science, 302 (2003) 875-878.

[11] (a) J.K. Jiang, K. Ghoreschi, F. Deflorian, Z. Chen, M. Perreira, M. Pesu, J. Smith, D.T. Nguyen, E.H. Liu, W. Leister, S. Costanzi, J.J. O'Shea, C.J. Thomas, Examining the chirality, conformation and selective kinase inhibition of 3-((3R,4R)-4-methyl-3-(methyl(7H-pyrrolo[2,3-d]pyrimidin-4-yl)amino)piperidin-1-yl)-3-oxopropanenitrile (CP-690,550), J Med Chem, 51 (2008) 8012-8018. (b) N.K. Williams, R.S. Bamert, O. Patel, C. Wang, P.M. Walden, A.F. Wilks, E. Fantino, J. Rossjohn, I.S. Lucet, Dissecting specificity in the Janus kinases: the structures of JAK-specific inhibitors complexed to the JAK1 and JAK2 protein tyrosine kinase domains, J Mol Biol, 387 (2009) 219-232. (c) M.I. Davis, J.P. Hunt, S. Herrgard, P. Ciceri, L.M. Wodicka, G. Pallares, M. Hocker, D.K. Treiber, P.P. Zarrinkar, Comprehensive analysis of kinase inhibitor selectivity, Nat Biotechnol, 29 (2011) 1046-1051. (d) M. Forster, A. Chaikuad, S.M. Bauer, J. Holstein, M.B. Robers, C.R. Corona, M. Gehringer, E. Pfaffenrot, K. Ghoreschi, S. Knapp, S.A. Laufer, Selective JAK3 Inhibitors with a Covalent Reversible Binding Mode Targeting a New Induced Fit Binding Pocket, Cell Chem Biol, 23 (2016) 1335-1340.

[12] B. Klunder, R.K. Mittapalli, M.F. Mohamed, A. Friedel, P. Noertersheuser, A.A. Othman, Population Pharmacokinetics of Upadacitinib Using the Immediate-Release and Extended-Release Formulations in Healthy Subjects and Subjects with Rheumatoid Arthritis: Analyses of Phase I-III Clinical Trials, Clin Pharmacokinet, 58 (2019) 1045-1058.

[13] M. Biggioggero, A. Becciolini, C. Crotti, E. Agape, E.G. Favalli, Upadacitinib and filgotinib: the role of JAK1 selective inhibition in the treatment of rheumatoid arthritis, Drugs Context, 8 (2019) 212595.

[14] F. Rivellese, A. Lobasso, L. Barbieri, B. Liccardo, A. de Paulis, FW. Rossi: Novel Therapeutic Approaches in Rheumatoid Arthritis: Role of Janus Kinases Inhibitors. Curr Med Chem. 2019;26(16):2823-2843.

[15] A. Thorarensen, M.E. Dowty, M.E. Banker, B. Juba, J. Jussif, T. Lin, F. Vincent, R.M. Czerwinski, A. Casimiro-Garcia, R. Unwalla, J.I. Trujillo, S. Liang, P. Balbo, Y. Che, A.M. Gilbert, M.F. Brown, M. Hayward, J. Montgomery, L. Leung, X. Yang, S. Soucy, M. Hegen, J. Coe, J. Langille, F. Vajdos, J. Chrencik, J.B. Telliez, Design of a Janus Kinase 3 (JAK3) Specific Inhibitor 1-((2S,5R)-5-((7H-Pyrrolo[2,3-d] pyrimidin-4-yl) amino)-2-methylpiperidin-1-yl)prop -2-en-1-one (PF-06651600) Allowing for the Interrogation of JAK3 Signaling in Humans. J. Med. Chem. 60 (2017) 1971-1993.

[16] J.B. Telliez, M.E. Dowty, L. Wang, J. Jussif, T. Lin, L. Li, E. Moy, P. Balbo, W. Li, Y. Zhao, K. Crouse, C. Dickinson, P. Symanowicz, M. Hegen, M.E. Banker, F. Vincent, R. Unwalla, S. Liang, A.M. Gilbert, M.F. Brown, M. Hayward, J. Montgomery, X. Yang, J. Bauman, J.I. Trujillo, A. Casimiro-Garcia, F.F. Vajdos, L. Leung, K.F. Geoghegan, A. Quazi, D. Xuan, L. Jones, E. Hett, K. Wright, J.D. Clark, A. Thorarensen, Discovery of a JAK3-Selective Inhibitor: Functional Differentiation of JAK3-Selective Inhibition over pan-JAK or JAK1-Selective Inhibition, ACS Chem. Biol. 11 (2016) 3442-3451.

[17] M. Kawamura, D.W. McVicar, J.A. Johnston, T.B. Blake, Y.Q. Chen, B.K. Lal, A.R. Lloyd, D.J. Kelvin, J.E. Staples, J.R. Ortaldo, et al., Molecular cloning of

L-JAK, a Janus family protein-tyrosine kinase expressed in natural killer cells and activated leukocytes, Proc. Natl. Acad. Sci. U S A, 91 (1994) 6374-6378.

[18] J.J. O'Shea, M. Pesu, D.C. Borie, P.S. Changelian, A new modality for immunosuppression: targeting the JAK/STAT pathway, Nat. Rev. Drug Discov. 3 (2004) 555-564.

[19] Y. Rochman, R. Spolski, W.J. Leonard, New insights into the regulation of T cells by gamma(c) family cytokines, Nat Rev Immunol, 9 (2009) 480-490.

[20] S.M. Russell, N. Tayebi, H. Nakajima, M.C. Riedy, J.L. Roberts, M.J. Aman, T.S. Migone, M. Noguchi, M.L. Markert, R.H. Buckley, J.J. O'Shea, W.J. Leonard, Mutation of Jak3 in a patient with SCID: essential role of Jak3 in lymphoid development, Science, 270 (1995) 797-800.

[21] J.D. Clark, M.E. Flanagan, J.B. Telliez, Discovery and development of Janus kinase (JAK) inhibitors for inflammatory diseases, J Med Chem, 57 (2014) 5023-5038.

[22] C. Liang, D. Tian, X. Ren, S. Ding, M. Jia, M. Xin, S. Thareja, The development of Bruton's tyrosine kinase (BTK) inhibitors from 2012 to 2017: A mini-review, Eur J Med Chem, 151 (2018) 315-326.

[23] L. Tan, K. Akahane, R. McNally, K.M. Reyskens, S.B. Ficarro, S. Liu, G.S. Herter-Sprie, S. Koyama, M.J. Pattison, K. Labella, L. Johannessen, E.A. Akbay, K.K. Wong, D.A. Frank, J.A. Marto, T.A. Look, J.S. Arthur, M.J. Eck, N.S. Gray, Development of Selective Covalent Janus Kinase 3 Inhibitors, J Med Chem, 58 (2015) 6589-6606.

[24] R.N. Yu, C.J. Chen, L. Shu, Y. Yin, Z.J. Wang, T.T. Zhang, D.Y. Zhang, Structure-based design and synthesis of pyrimidine-4,6-diamine derivatives as Janus kinase 3 inhibitors, Bioorg. Med. Chem. 27 (2019) 1646-1657.

[25] Y. Yin, C.J. Chen, R.N. Yu, Z.J. Wang, T.T. Zhang, D.Y. Zhang, Structure-based design and synthesis of 1H-pyrazolo[3,4-d]pyrimidin-4-amino derivatives as Janus kinase 3 inhibitors, Bioorg. Med. Chem. 26 (2018) 4774-4786.

[26] Y. Yin, C.J. Chen, R.N. Yu, L. Shu, T.T. Zhang, D.Y. Zhang, Discovery of novel selective Janus kinase 2 (JAK2) inhibitors bearing a 1H-pyrazolo[3,4-d]pyrimidin-4-amino scaffold, Bioorg. Med. Chem. 27 (2019) 1562-1576.

[27] M. Hu, C.B. Xu, C. Yang, H.L. Zuo, C.J. Chen, D. Zhang, G.N. Shi, W.J. Wang, J.G. Shi, T.T. Zhang, Discovery and evaluation of ZT55, a novel highly-selective tyrosine kinase inhibitor of JAK2V617Fagainst myeloproliferative neoplasms, J. Exp. Clin. Cancer Res. 38 (2019) 49.

[28] J.W. Tyner, T.G. Bumm, J. Deininger, L. Wood, K.J. Aichberger, M.M. Loriaux, B.J. Druker, C.J. Burns, E. Fantino, M.W. Deininger, CYT387, a novel JAK2 inhibitor, induces hematologic responses and normalizes inflammatory cytokines in murine myeloproliferative neoplasms, Blood, 115 (2010) 5232-5240.

[29] Y. Li, T. Ye, L. Xu, Y. Dong, Y. Luo, C. Wang, Y. Han, K. Chen, M. Qin, Y. Liu, Y. Zhao, Discovery of 4-piperazinyl-2-aminopyrimidine derivatives as dual inhibitors of JAK2 and FLT3, Eur J Med Chem, 181 (2019) 111590.

[30] S. Nuhaily, B. Damaj, A. Maghazachi, Oxazolone-Induced Delayed Type Hypersensitivity Reaction in the Adult Yucatan Pigs. A Useful Model for Drug Development and Validation, Toxins, 1 (2009) 25-36.

[31] Y. Fujii, T. Sengoku, Effects of the Janus kinase inhibitor CP-690550 (tofacitinib) in a rat model of oxazolone-induced chronic dermatitis, Pharmacology, 91 (2013) 207-213.

[32] D.M. Wang, M. Hu, X.P. Li, D. Zhang, C.J. Chen, J.M. Fu, S.A. Shao, G.N. Shi, Y. Zhou, S. Wu, T.T. Zhang, Design, synthesis, and evaluation of isoflavone analogs as multifunctional agents for the treatment of Alzheimer's disease, Eur. J. Med. Chem. 168 (2019) 207-220.

- Compound **12 is** a potent JAK3 inhibitor (IC_{50} = 1.7 nM), highly selective vs JAK1 (x 777) and JAK2 (x 588).
- Compound **12** obviously inhibited the JAK3-dependent signaling and T cell proliferation.
- Compound **12** suppressed the oxazolone-induced delayed type hypersensitivity responses in mice.
- Compound **12** displayed moderate pharmacokinetic properties and is suitable for *in vivo* use.

Declaration of interests

☒ The authors declare that they have no known competing financial interests or personal relationships that could have appeared to influence the work reported in this paper.

☐The authors declare the following financial interests/personal relationships which may be considered as potential competing interests: